

# Dip Coating of Metal Implants with Antibacterial Polymer Matrix for the Prevention of Implant Associated Infections

Submitted to the Graduate School of Natural and Applied Sciences  
in partial fulfillment of the requirements for the degree of

Master of Science

in Biomedical Engineering

by

Emine Hilal Altıntop

ORCID 0009-0004-3766-1918

Advisor: Assoc. Prof. Dr. Didem Şen Karaman

February, 2024

This is to certify that we have read the thesis **Dip Coating of Metal Implants with Antibacterial Polymer Matrix for the Prevention of Implant Associated Infections** submitted by **Emine Hilal Altıntop**, and it has been judged to be successful, in scope and in quality, at the defense exam and accepted by our jury as a MASTER'S THESIS.

**APPROVED BY:**

**Advisor:**

**Assoc. Prof. Dr. Didem Şen Karaman**  
İzmir Kâtip Çelebi University

**Committee Members:**

**Assoc. Prof. Dr. Didem Şen Karaman**  
İzmir Kâtip Çelebi University

**Assoc. Prof. Dr. Utku Kürşat Ercan**  
İzmir Kâtip Çelebi University

**Assist. Prof. Dr. Esra Kasapgil**  
Bakircay University

**Date of Defense: February 01, 2024**

# Declaration of Authorship

I, **Emine Hilal Altıntop**, declare that this thesis titled **Dip Coating of Metal Implants with Antibacterial Polymer Matrix for the Prevention of Implant Associated Infections** and the work presented in it are my own. I confirm that:

- This work was done wholly or mainly while in candidature for the Master's / Doctoral degree at this university.
- Where any part of this thesis has previously been submitted for a degree or any other qualification at this university or any other institution, this has been clearly stated.
- Where I have consulted the published work of others, this is always clearly attributed.
- Where I have quoted from the work of others, the source is always given. This thesis is entirely my own work, with the exception of such quotations.
- I have acknowledged all major sources of assistance.
- Where the thesis is based on work done by myself jointly with others, I have made clear exactly what was done by others and what I have contributed myself.

Date: 01.02.2024

---

# Dip Coating of Metal Implants with Antibacterial Polymer Matrix for the Prevention of Implant Associated Infections

## Abstract

The recent increase in life expectancy and changing living conditions have led to a rise in developments regarding implants, particularly in orthopedic implants. It is important to note that this statement is based on objective evidence and not subjective evaluations. Despite these advances, issues with metallic implants such as Ti, Ti alloy, Co-Cr alloy, and stainless steel (AISI 316L), which are currently preferred, persist. There are several limitations to implant materials, including corrosion due to the physiological environment, bacterial infection, and biofilm formation. Although these limitations have not been extensively studied, they prevent the attainment of the desired level of implant material and result in a lifespan of approximately 20 years for currently used implants.

Despite their biocompatibility and biohardness, implant-related infections can occur due to bacterial colonization. *Staphylococcus aureus* is known to colonise foreign bodies and increase the risk of implant-related infection. Infections caused by *S. aureus* can delay the healing process, cause bone loss, and require long-term antibiotic use. It is widely accepted that 40% of *S. aureus* strains are resistant to antibiotics. The development of drug resistance can increase and lead to implant replacement, which may result in infections and even death. Negative changes in implant performance often occur due to reactions between the implant and surrounding tissue, which are caused by the physical and chemical properties of the

implant surface. Therefore, modifying the surface properties of materials, both chemically and physically, shows great potential in improving implant integration. Additionally, with the rise of antibiotic-resistant infections and limited treatment options, there is growing interest in integrating antibacterial properties into biomaterials.

Coating technologies are preferred for overcoming the limitations associated with implants. These include plasma spraying, biomimetic deposition, electrochemical deposition, electrophoretic deposition, and sol-gel coating. The primary goal of these coating technologies is to increase biocompatibility and create an antibacterial effect. Complex organic, inorganic, or hybrid materials, using a combination of these two, are preferred for implant coatings. Polymers and metal/metal oxide nanoparticles are examples of organic and inorganic materials, respectively.

This study aims to create a surface coating for K-Wires using the dip coating or sol-gel method. The coating matrix use polyvinyl alcohol (PVA) due to its economic and solubility advantages. PVA is a preferred polymer for implant surface adhesion. Quaternary ammonium silanes (QAS) are inorganic materials that possess antibacterial properties. When combined with PVA, these hybrid materials can provide antimicrobial properties without the need for additional binders. Due to their low toxicity and antibacterial properties, QAS can be a preferred material for preventing post-implantation infections.

**Keywords:** Dip coating, QAS, PVA, Antimicrobial, K-Wire

# İmlantla İlişkili Enfeksiyonların Önlenmesi İçin Metal İmplantların Antibakteriyel Polimer Matrisli Daldırma Kaplaması

## ÖZ

Son zamanlarda ki yaşam beklentisinin artması ve yaşam şartlarının değişmesi ile birlikte implantlarla ilgili gelişmelerde artmaktadır. Özellikle bu artış ortopedik implantlarda yaşanmaktadır. Şu anda özellikle tercih edilen Ti, Ti alaşımı, Co-Cr alaşımı ve paslanmaz çelik (AISI 316L) gibi metalik implantlarla ilgili sorunlar tüm bu ilerlemelere rağmen hala devam etmektedir. Fizyolojik ortamdan kaynaklı korozyonların meydana gelmesinden bakterilerle ilgili enfeksiyon ve biyofilm oluşumuna kadar bir çok sınırlamalar mevcuttur. Bu sınırlamalar üzerine çalışmalar yapılsa da istenilen düzeyde implant malzemesi elde edilememiştir ve şu anda kullanılan implanların yaklaşık ömrü 20 yıl kadardır. Ancak implant malzemelerinin biyoyumluluğuna ve biyolojik sertliğine rağmen bakteriyel kolonizasyon ve ardından implantla ilişkili enfeksiyonlar meydana gelebilir. Özellikle *S. aureus*'un yabancı cisimleri kolonize ettiği ve implantla ilişkili enfeksiyon riskini arttırdığı bilinmektedir. *S. aureus*'un neden olduğu enfeksiyonlar iyileşme sürecini geciktirebilir, kemik kaybına neden olabilir ve uzun süreli antibiyotik kullanımını gerektirebilir. *S. aureus* suşlarının %40'ının antibiyotiklere dirençli olduğu yaygın olarak kabul edilmektedir. Sonuç olarak, ilaç direncinin gelişimi artmakta, implantın değiştirilme olasılığı artmakta ve amputasyon ve hatta ölümlerle sonuçlanabilecek enfeksiyonlara yol açabilmektedir. İmplant performansındaki olumsuz gelişmeler çoğu zaman implant ile çevre doku arasındaki reaksiyonlardan kaynaklanmaktadır.

Bu reaksiyonlar tipik olarak implant yüzeyinin fiziksel ve kimyasal özelliklerinden kaynaklanmaktadır. Bu nedenle, malzemelerin yüzey özelliklerinin hem kimyasal hem de fiziksel olarak değiştirilmesi, implant entegrasyonunu arttırmada büyük umut vaat etmektedir. Eş zamanlı olarak, antibiyotiğe dirençli enfeksiyonlar arttıkça ve tedavi seçenekleri sınırlandıkça, antibakteriyel özelliklerin biyomateryallere dahil edilmesine olan ilgi de artıyor.

İmplantlar ilişkili sınırlamaların üstesinden gelmek için kaplama teknolojileri tercih edilmektedir. Bunlar plazma püskürtme, biyomimetik biriktirme, elektrokimyasal biriktirme, elektroforetik biriktirme, sol-jel kaplama şeklinde sıralanabilir. Bu kaplama teknolojileri ile biyoyumuluğu arttırmak ve antibakteriyel etki oluşturmak öncelikli hedef haline gelmiştir. İmplant kaplamaları için oluşturan kompleksler organik, inorganik veya bu ikisinin birleşiminin kullanıldığı hibrit malzemeler tercih edilmektedir. Organik olanlara polimerler, inorganik olanlara ise metal ve metal oksit nanoparçacıklar örnek verilebilir.

Sonuç olarak bu çalışmada sol jel kaplama yönteminin daldırma kaplama metodu ile K-Wirelar için yüzey kaplaması oluşturulacaktır. Kaplama matrisinde hem ekonomik açıdan hem de çözünürlük açısından avantajlı olan PVA tercih edilecektir. PVA kaplama solüsyonunun implant yüzeyine yapışmasında tercih edilen bir polimer olmuştur. Antibakteriyel özellik açısından inorganik malzeme olan QAS tercih edilmiştir. Bu iki hibrit malzeme olan PVA ve QAS birlikte kullanıldığında bağlayıcı olarak herhangi bir etken maddeye ihtiyaç duymadan antimikrobiyal özellikler elde edilebilmektedir. Bu özellikleri ve düşük toksisiteleri nedeniyle, implantasyon sonrası enfeksiyonların üstesinden gelmeye yardımcı olacak ve bakterisidal özellikler sağlayacak bir malzeme olarak QAS tercih edilebilir.

**Anahtar Kelimeler:** Daldırma Kaplama, QAS, PVA, Antimikrobiyal, K-Wire



*To my lovely family...*

# Acknowledgment

I would like to express my gratitude to my advisor, Assoc. Prof. Dr. Didem ŐEN KARAMAN, for her patient and tolerant support throughout this study. Additionally, I am thankful for the opportunities provided to me.

I would like to thank my laboratory mate, Beyzanur DOĐRUYOL, for her moral support and assistance with the experiments. Finally, I would like to thank Aylin KORKMAZ, Elif YÜZER and Merve OĐUZ for their work and support.

I would like to express my endless gratitude to Damla SOYLU for supporting me throughout the process of completing this thesis and helping me overcome all difficulties.

My deepest appreciation goes to my family...

# Table of Contents

Declaration of Authorship .....	ii
Abstract .....	iii
Öz.....	v
Acknowledgment .....	viii
Table of Contents .....	ix
List of Figures.....	xii
1. Introduction.....	1
1.1 Implant Infection.....	1
1.2 Orthopedic Implant-Associated Staphylococcal Infections .....	3
1.3 Type of Coatings .....	7
1.3.1 Plasma Spraying .....	8
1.3.2 Biomimetic Deposition .....	8
1.3.3 Electrochemical Deposition .....	9
1.3.4 Electrophoretic Deposition.....	11
1.3.5 Sol-gel Coating .....	12
2. Materials and Methods .....	16
2.1 Preparation of Coating Solutions .....	16
2.1.1 Preparation of Polyvinyl Alcohol (PVA) Phase .....	16

2.1.2	Mixing of Silane Content with PVA Solution .....	16
2.2	Dip Coating Process .....	17
2.3	Characterization of Dip Coated Surfaces .....	17
2.3.1	Rheological Analysis .....	17
2.3.2	Scanning Electron Microscope (SEM) Analysis .....	18
2.3.3	Surface Cation Density ( $\text{NH}_4/\text{cm}^2$ ) Analysis .....	18
2.3.4	Contact Angle .....	19
2.3.5	Raman Spectrometry Analysis .....	19
2.4	<i>In vitro</i> Studies and Cytotoxicity Studies .....	20
2.4.1	<i>In vitro</i> Antibacterial Studies .....	20
2.4.2	<i>In Vitro</i> Cytocompatibility Investigations .....	22
3.	Result and Discussion .....	24
3.1	Characterization of Coating Surfaces .....	24
3.1.1	Rheological Analysis .....	24
3.1.2	Scanning Electron Microscope (SEM) Analysis .....	25
3.1.3	Surface Cation Density ( $\text{NH}_4/\text{cm}^2$ ) Analysis .....	28
3.1.4	Contact Angle .....	29
3.1.5	Raman Spectrometry Analysis .....	30
3.2	<i>In vitro</i> Studies and Cytotoxicity Studies .....	31
3.2.1	Bacterial Cell Adhesion Research on K- Wire .....	31
3.2.2	Investigation of <i>In vitro</i> Antibiofilm Effect .....	35
3.2.3	<i>In vitro</i> Cytocompatibility Results .....	37

4. Conclusion .....	39
References .....	40
Curriculum Vitae .....	49



# List of Figures

Figure 3. 1: Rheological analysis of (a) Stress Curve and (b) Viscosity Curve of PVA-TEOS, where condensation reactions take place .....	24
Figure 3. 2: Rheological analysis of (a) Stress Curve and (b) Viscosity Curve of PVA-TEOS-QAS, where condensation reactions take place .....	25
Figure 3. 3: SEM analysis of (a) 100 mm/min 1x 30sec, (b) 100 mm/min 1x 60 sec, (c) 100 mm/min 3x 30 sec (d) 100 mm/min 3x 60 sec of glass lam surface coatings performed at different drawing speeds, single layer and triple layer and different waiting times .....	26
Figure 3. 4: Light microscope image of the coatings applied on the glass lam surface a) 40 mm/min 1x 60sec, (b) 100-80 mm/min 2x 30-60 sec .....	26
Figure 3. 5: SEM analysis of PVA-TEOS coatings applied on glass lam surface in one layer and two layers at different waiting times at a constant speed (a) 50 mm/min 1x 60 sec, (b) 50 mm/min 1x 80 sec, (c) 50 mm/min. min 1x 99 sec (d) 50 mm/min 2x 60 sec (e) 50 mm/min 2x 80 sec, (f) 50 mm/min 2x 99 sec .....	27
Figure 3. 6: SEM images of the determination of the surface topology and thickness of the coatings applied to the glass lam surface (a) PVA-TEOS, (b) PVA-TEOS-QAS, (c) PVA-TEOS-QAS T.....	28
Figure 3. 7: Contact angle measurement of the coated surface and samples made with coating solutions (a) Glass, (b) PVA-TEOS, (c) PVA-TEOS-QAS.....	30
Figure 3. 8: Hydrolysis and condensation reactions were completed PVA-TEOS and incorporated into the coating matrix of QAS, and Raman Spectrometry analysis was performed (a) Si-O-Si Bond, (b) Ammonium Salts.....	31

Figure 3. 9: Viability of *S. aureus* cells on K-Wires coated with as determined CTRL, NC Wire, PVA-TEOS, PVA-TEOS-QAS by coloni counting. (p value style: GP: 0,1234 (ns), 0,0332(\*), 0,0021(\*\*), 0,0002(\*\*\*), <0,0001(\*\*\*\*),One-way ANOVA) .....32

Figure 3. 10: Viability of *S. aureus* cells on K-Wires coated with as determined CTRL, NC Wire, PVA-TEOS, PVA-TEOS-QAS by Alamar blue assay. (p value style: GP: 0,1234 (ns), 0,0332(\*), 0,0021(\*\*), 0,0002(\*\*\*), <0,0001(\*\*\*\*),One-way ANOVA) .....33

Figure 3. 11: Viability of adhered *S. aureus* cells on K-Wires coated with as determined NC Wire, PVA-TEOS, PVA-TEOS-QAS by coloni counting. (p value style: GP: 0,1234 (ns), 0,0332(\*), 0,0021(\*\*), 0,0002(\*\*\*), <0,0001(\*\*\*\*)).....34

Figure 3. 12: Viability of adhered *S. aureus* cells on K-Wires coated with as determined NC Wire, PVA-TEOS, PVA-TEOS-QAS by Alamar Blue assay. (p value style: GP: 0,1234 (ns), 0,0332(\*), 0,0021(\*\*), 0,0002(\*\*\*), <0,0001(\*\*\*\*)).....35

Figure 3. 13: The bacterial cell viability of formed *S. aureus* biofilm on NC Wire, PVA-TEOS, PVA-TEOS-QAS was determined by Alamar blue assay. (p value style: GP: 0,1234 (ns), 0,0332(\*), 0,0021(\*\*), 0,0002(\*\*\*), <0,0001(\*\*\*\*)) .....36

Figure 3. 14: The effect of biomass of *S. aureus* biofilm on NC Wire, PVA-TEOS, PVA-TEOS-QAS was determined with Crystal Violet. (p value style: GP: 0,1234 (ns), 0,0332(\*), 0,0021(\*\*), 0,0002(\*\*\*), <0,0001(\*\*\*\*)) .....37

Figure 3. 15: NC Wire, PVA-TEOS, PVA-TEOS-QAS toxicity tests were performed with L929 cell line and cell viability testing was performed with Alamar blue assay. (p value style: GP: 0.1234 (ns), 0.0332(\*), 0.0021(\*\*), 0.0002(\*\*\*), <0.0001(\*\*\*\*)) .....38

# List of Abbreviations

Ti	Titanium
Co- Cr	Cobalt- Chrome
AISI 316L	Stainless Steel
K-Wire	Kirschner Wire
<i>S. Aureus</i>	<i>Staphylococcus Aureus</i>
DNA	Deoxyribose Nucleic Acid
m-RNA	messenger ribonucleic acid
MSCRAMM	microbial surface components that recognise adhesive matrix molecules
LPS	Lipopolysaccharides
MRSA	Methicillin-resistant <i>S. Aureus</i>
ESCAPE	<i>Enterococcus faecium</i> , <i>S. aureus</i> , <i>Klebsiella pneumoniae</i> , <i>Acinetobacter baumannii</i> , <i>Pseudomonas aeruginosa</i> , and
CDC	Centers for Disease Control
MDR	multidrug-resistant
FDA	The Food and Drug Administration
HA	Hydroxyapatite
BSA	Bovine Serum Albumin
ECM	Extracellular Matrix
pDA	polydopamine
SBF	Simulated Body Fluid
AgNP	Silver Nanoparticle

Ag	Silver
Cu	Copper
ZnO	Zinc Oxide
ECD	Electrochemical deposition
EPD	Electrophoretic deposition
QAC	Quaternary Ammonium Compounds
AMP	Antimicrobial Peptides
AME	Antimicrobial Enzymes
PVA	Polyvinyl Alcohol
QAS	Quaternary ammonium silanes
TEOS	Tetraethyl Orthosilicate
HNO <sub>3</sub>	Nitric Acid
NaOH	Sodium hydroxide
SEM	Scanning Electron Microscope
NH <sub>4</sub>	Ammonium
TSA	Tryptic Soy Agar
RPM	Revolutions Per Minute
PBS	Phosphate Buffered Saline
DMEM	Dulbecco's Modified Eagle Medium
FBS	Fetal Bovine Serum

# List of Symbols

m	Mass [kg]
mL	Milliliter
$\mu\text{L}$	Microliter
Nm	Nanometer
$^{\circ}\text{C}$	Celsius Degree
M	Molar
Mm	Millimeter

# Chapter 1

## 1. Introduction

### 1.1 Implant Infection

In recent times, the rise in life expectancy and changes in lifestyle have contributed to a significant increase in the number of surgical implant treatments. With the rise in demand for enhanced performance of medical devices coupled with advancements in technology, the biomedical and biomaterial industry has led significant growth and expansion in recent years. Today, approximately 1.5 million joint replacements are performed annually in Europe and 7 million in the United States[1]. Based on this, it is seen that the mentioned case is more related to the devices used in orthopedic surgery[2]. Metallic materials such as Ti, Ti alloy, Co-Cr alloy and stainless steel (AISI 316L) are predominantly preferred over ceramic and polymeric materials in implants due to their high fatigue resistance and high strength. Titanium and its alloys, for example, are widely preferred in hard tissue construction due to their biocompatibility, good mechanical properties, low Young's modulus, non-magnetic behavior, good resistance to corrosion and light weight [3, 4] . Another example is the use of stainless steel in many implant applications such as bone screws and fracture plates. However, it has often been reported that stainless steel is subject to cracking and galvanic corrosion due to the nature of the physiological environment. When stainless steel corrodes, metal ions are released, which can cause systemic effects and lead to the loosening of the implant[3]. Implant failure can be caused by negative immune system reactions, biofilm formation, and biocompatibility issues. These factors can lead to a range of problems, including implant rejection and other complications[1]. However, despite numerous studies aimed at improving and developing existing biomaterials, they have not yet been produced to the desired level in terms of mechanical, chemical, and biocompatibility properties. Based on

this, the lifespan of implants used today might reduce. This increases the need for implant revision, particularly for young patients, which poses economic and social challenges[1]. However, despite the biocompatibility and biorigidity of implant materials, bacterial colonization and subsequent implant-related infections can occur. *S. aureus*, in particular, is known to colonise foreign bodies and increase the risk of implant-related infections[5]. Infections caused by *S. aureus* can delay the healing process, cause bone loss, and require long-term antibiotic use. It is widely recognised that 40% of *S. aureus* strains are resistant to antibiotics[6]. Consequently, the development of drug resistance increases, the likelihood of implant replacement and may lead to infections that could result in amputation or even death [6]. Negative developments in implant performance are often caused by reactions between the implant and the surrounding tissue. These reactions are typically due to the physical and chemical properties of the implant surface. Therefore, modifying the surface properties of implant materials, both chemically and physically, shows great promise in enhancing implant integration[1]. Simultaneously, as antibiotic-resistant infections are on the rise and treatment options become limited, there is growing interest in incorporating antibacterial properties into biomaterials[7].

Osteogenic implants, alternatively referred to as trauma implants, are orthopedic prostheses that are employed to mend and realign fractured bones. Implants used in orthopaedic surgeries are categorised into two groups: external and internal. Internal fixators are utilised in the treatment of fractures, and can include plates, screws, nails, rods, wires and pins. They aid in the healing of fractured structures by limiting movement during the treatment of fracture processes. Bioinert materials, rather than bioactive ones, are generally preferred for these implants as tissue adhesion is not desired. External implants are inserted into the body through a small incision outside the body. They have minimal impact on soft tissue damage and can be adjusted after placement. However, they have limitations, such as the risk of malunion in fractures. Therefore, external implants are typically preferred for short-term treatments that do not require surgery[8]. Introduced by Martin Kirschner in 1909, Kirschner wires, also known as K-wires, are commonly used in orthopaedic and veterinary surgery to hold bone fragments together (pin fixation) or for skeletal traction. K-Wires are easy to place, cause minimal damage to soft tissues such as tendons and neurovascular structures, and are cut and fixed so that they remain outside the tissue[9]. Given the

various applications of K-wires, they may serve as a possible route for bacteria to travel from the skin to the bone, leading to infection[7]. For instance, the occurrence of infection in hand and wrist fractures ranges from 1.9% to 34% [9]. Superficial infections can be treated with regular dressings or oral antibiotics. However, in more severe cases, the pin may need to be removed, which can lead to complications if the fracture has not healed. Hospitalization for intravenous antibiotic therapy or further surgery may be necessary for more severe infections such as osteomyelitis [9].

## 1.2 Orthopedic Implant-Associated Staphylococcal Infections

The presence of a foreign body triggers bacterial colonisation and initiates competition between bacterial cells and tissue cells, according to the surface race theory. The presence of a foreign body triggers bacterial colonisation and initiates competition between bacterial cells and tissue cells, according to the surface race theory. If the tissue cells win the race, colonisation is less likely to occur. However, if the bacterial cells win, bacterial toxins disrupt the structure of the tissue cells [10]. The adhesion of bacterial and tissue cells to biomaterial surfaces is typically evaluated using the same method. The number of bacterial cells may initially increase, leading to a decrease in host cell numbers [11].

*S. aureus* is a gram-positive pathogen that causes numerous human infections. Critical to surface recognition and adhesion is the presence of microbial surface components that recognise adhesive matrix molecules on the membrane of *S. aureus*. Biophysically, the attachment of bacteria to surfaces is a two-stage process. The first stage is cell-surface interaction, where mostly non-specific forces are effective. The second stage is secondary short-range interactions, where a specific bond is formed. After the formation of the secondary bond, cell-surface coupling is experienced at higher levels, and mechanical and chemical effects are needed to destroy the bacteria [12].

The colonisation of host tissue and spread to other sites by *S. aureus* is dependent on the production of various virulence factors. These factors consist of helper

cytoplasmic, surface, and secreted components that are regulated at the transcriptional level in response to endogenous and environmental cues, such as cell density, pH, and sub-inhibitory concentrations of antibiotics [13]. In cases of such infections, high-dose and long-term antibiotic treatment is necessary. However, it is unfortunate that the implant material must be surgically removed after prolonged antibiotic treatment[14].

The use of antibiotics greatly improved human health in various areas, including orthopaedic surgery and implant results. Prior to their use, infections caused by *S. aureus* often resulted in death or amputation. Antibiotics significantly reduced the number of fatalities and surgical procedures, leading to an improvement in people's living standards. Over the years, the discovery, proliferation, and misuse of antibiotics have facilitated the emergence of antibiotic-resistant bacteria. Recently, antibiotic production has decreased considerably due to government policies and the uncertain life cycle of antibiotics. Antibiotic resistance has been discovered shortly after the discovery of new antibiotics. Methicillin was introduced in 1959 and Methicillin-resistant *S. Aureus* (MRSA) was identified in 1961. Since then, MRSA has become the leading cause of hospital-acquired infections and has spread worldwide, leading to antibiotic resistance being recognised as a major threat to human health. The antibiotic-resistant bacteria currently described include *Enterococcus faecium*, *S. aureus*, *Klebsiella pneumoniae*, *Acinetobacter baumannii*, *Pseudomonas aeruginosa*, and *Enterobacter microorganisms*, collectively known as 'ESKAPE'. These microorganisms cause significant mortality and morbidity. In the United States, the Centers for Disease Control and Prevention (CDC) has categorized multidrug-resistant (MDR) organisms into three threat categories: immediate, severe, and alert [15].

Multidrug-resistant strains of *S. aureus* acquire resistance through three internal mechanisms. The first mechanism is the reduction of permeability of the outer membrane. When the permeability of the cell membrane decreases, bacteria are affected, and drug permeability also decreases. For instance, the resistance of *S. aureus* to aminoglycosides is caused by membrane permeability, and drug resistance is achieved in this way. Secondly, in efflux systems, genes that activate efflux systems are activated after stimulation by substrates in the environment, and the

ability to expel drugs is gained, and this is how drug resistance occurs. There are three types of drug pumping proteins for *S. aureus*: QacA, NorA, and Smr. QacA is also considered to be a significant factor in MRSA. Excessive  $\beta$ -Lactamase Production is an enzyme that catalyses the hydrolysis of  $\beta$ -lactam antibiotics and is coded by bacterial chromosomal genes.  $\beta$ -lactam antibiotics cause bacterial death in two ways, and  $\beta$ -Lactamase inactivates antibiotics in two ways: firstly, by hydrolysing the antibiotics, and secondly, by secreting excessive  $\beta$ -Lactamase, which compresses and prevents the antibiotics from passing into the intracellular space. This results in the development of antibiotic resistance in MRSA [16].

Another resistance mechanism is acquired resistance, which is obtained through mutation or horizontal gene transfer from a previously susceptible bacterium. Horizontal gene transfer occurs in three ways, one of which is transformation. Transformation is a form of genetic recombination where free DNA fragments from a dead bacterium enter the recipient bacterium and are incorporated into its chromosome. Only a few bacteria can be naturally transformed. Transformation involves the uptake of free DNA fragments from a dead bacterium by a recipient bacterium, which are then incorporated into its chromosome. This fragment describes three mechanisms of horizontal gene transfer in bacteria: transformation, transduction, and conjugation. Transduction, on the other hand, involves the transfer of genetic material between a donor and a recipient bacterium by a bacteriophage. Finally, conjugation is considered the most important mechanism of horizontal gene transfer. This process involves the transfer of genetic material from one bacterial cell to another through direct physical contact between the cells [17].

Adaptive resistance is the resistance to one or more antibiotics induced by a specific environmental signal, such as stress, growth status, pH, ion concentrations, nutritional conditions, or lower inhibitory levels of antibiotics. The resistance mechanism may be epigenetic rather than genetic. It can be restored when the stimuli are removed, but a gradual increase in the MIC value of the antibiotic can be observed [17].

*S. aureus* cause a variety of infections [18]. The formation of bacterial biofilms is significant in initiating infectious processes around implant surfaces. In implant-related infections, bacterial attachment and biofilm formation may vary depending on

the microorganism species and implant surface characteristics. For instance, it has been observed that biofilm-forming strains exhibit greater adhesion than non-biofilm-forming strains. *S. aureus* colonises or adheres differently depending on whether it forms a biofilm or an adhesive layer on the implant. Additionally, differences in implant surface topography, such as micro-roughened and electropolished surfaces, may affect *S. aureus* adhesion. The ability of *S. aureus* to adhere to components of the extracellular matrix and to plasma proteins deposited on the surface of biomaterials can ultimately lead to the formation of a biofilm, which is the major cause of implant-related infections [19].

Biofilm formation occurs in three stages: initial adhesion to the surface, microcolony formation, and biofilm maturation through the separation of bacteria. During the first step of biofilm formation in the human body, *S. aureus* expresses several microbial surface components that recognize and bind to extracellular matrix molecules, such as fibrinogen and fibronectin proteins [14]. On the positive side, the plasma proteins that adhere to the surface of the implant provide a physiological environment for the adaptation to the host tissue [20]. Matrix proteins can also be adsorbed to the surface of medical devices after implantation and become targets for specific binding to staphylococcal surface components, providing an excellent scaffold for colonisation and infection [14, 20]. For this purpose, bacteria have evolved a number of surface-associated proteins called MSCRAMM (microbial surface components that recognise adhesive matrix molecules), each binding to a specific set of host proteins. The most widespread group of surface proteins that bind to extracellular matrix and plasma proteins is the MSCRAMM protein family. Protein A (SpA) is an important MSCRAMM that is expressed at high levels in *S. aureus* [21].

Reversible interactions, driven by physical forces such as van der Waals forces and steric-electrostatic interactions, are responsible for initial bacterial adhesion to surfaces. Bacterial cells then bind irreversibly to substrates through hydrogen bonds, ionic bonds and dipole-hydrophobic interactions. Bacterial cell surface structures, including lipopolysaccharides (LPS) and exopolysaccharides, play a role in these interactions [14]. Once attached to the plasma protein-coated device, the bacteria multiply, grow and produce polymeric molecules to form an extracellular matrix. Biofilm polymers include polysaccharides, proteins, extracellular DNA (eDNA),

teichoic acids and other molecules. They form an aqueous gel-like material with favourable mechanical properties and resistance to external impacts [20].

Treatment of *S. aureus* infections is typically limited to conventional antibiotics, but failures are common due to the emergence of antibiotic-resistant strains, as well as intrinsic antibiotic resistance following biofilm formation. The biofilm is composed of several layers of bacteria that are coated and interconnected in an extracellular matrix, forming a complex three-dimensional structure. This structure protects against host defences and limits the therapeutic efficacy of all available antibiotics [18]. Therefore, new and effective anti-biofilm antibiotics must be able to penetrate the biofilm structure and have a high level of antimicrobial resistance[20] .

### 1.3 Type of Coatings

Recently, over 90% of the elderly population has been affected by bone and bone-related disorders. Therefore, there is a need for implant materials that possess specific properties, such as high biocompatibility, durability, low elastic modulus, and high strength. Metallic implants, particularly Ti implants and alloys, meet most of these requirements. However, titanium implants still have limitations. For example, they can leave residues that lead to bone resorption, or there is a high risk of infection after implantation.

To overcome these limitations and achieve the desired properties, surface modifications can be applied. Recently, bioinert and bioactive coatings have been used, with bioactive HAp being the most favoured. The Food and Drug Administration (FDA) describes the coating conditions, which must meet properties such as thickness, crystallinity, phase purity, Ca/P ratio, density, heavy metals, tensile resistance, shear strength, and abrasion. While various methods, including sol-gel coating, plasma spraying, biomimetic deposition, electrochemical deposition, and electrophoretic deposition, are found in the literature, only plasma spraying is commercially approved by the FDA [22].

Coating types can be listed as follows; plasma spraying, biomimetic deposition, electrochemical deposition, electrophoretic deposition, sol-gel coating. In addition, sol-gel coating is divided into three types: spray coating, spin coating and dip coating.

### 1.3.1 Plasma Spraying

The basic principle of the plasma spray coating technique consists of heating HAp particles at very high temperatures with the plasma flame generated by the electrical discharge between the electrodes. The process involves depositing molten HAp particles onto the substrate surface, which are then rapidly cooled to form a coating layer [23]. This technique has been observed to provide a strong interface between the coating and the alloy, promoting bone growth and mineralisation [24].

However, plasma sprayed HA coatings face challenges such as phase separation and amorphous phase formation. For instance, the high temperature has been observed to cause the formation of undesired phases such as  $\alpha/\beta$ -TCP or CaO/TTCP [25]. Nevertheless, new methods have been attempted to overcome these limitations [24, 25].

### 1.3.2 Biomimetic Deposition

Researchers have recently developed various types of coatings to increase the biocompatibility and lifespan of implants, as well as to prevent bacterial colonization and biofilm formation. Biomimetic coatings have been extensively studied for their potential in improving implant success rates and for their strong antimicrobial properties [26, 27].

Biodegradable nanoparticles based on bovine serum albumin (BSA) are an excellent choice for drug delivery due to their high transport efficiency and biocompatibility. These nanoparticles can overcome coating limitations that lead to antibacterial resistance or toxic effects, such as physical adsorption, chemical grafting, polymer coating containing antibacterial drugs, and silver-containing coatings.

Creating a biomimetic natural extracellular matrix (ECM) microenvironment on the surface of bone implants has been a recent focus. This is due to the demonstrated ability of ECM proteins to regulate cell adhesion, proliferation, and differentiation. Another biomimetic coating, inspired by natural mussel chemistry, is polydopamine (pDA), which effectively facilitates adhesion to the material surface through adhesive proteins [28].

To achieve compatibility with bone tissue, a coating must be applied to the metal implant surface. HA and calcium phosphate coatings are widely used to improve the compatibility between hard tissue and metal implants. Biomimetic approaches that imitate the mineralisation process of bone to produce calcium phosphate coatings have gained significant attention due to their effectiveness. Supersaturated aqueous solutions with an ionic composition similar to that of human plasma are the preferred method for coating complex-shaped materials. Simulated body fluid calcification solution (SBF) is widely recommended in the literature for this purpose [27].

Another biomimetic method is to use silk fibroin from the *Bombyx mori* silkworm to make a coating by mixing AgNP, which is favored as an antibacterial, with gentamicin, which has been shown to have a synergistic effect. Because of its capacity to recognize substrates and be biocompatible, SF is typically chosen in biomedical coatings [29].

Sharklet micro-patterned surfaces are a spectacular illustration of the biomimetic technique. The goal here is to either prevent bacterial adhesion with micro and nanotopography or to destroy bacteria through contact. The wing biomimetry of the cicada (*Psaltoda claripennis*) fly is equally efficient against Gram-positive and Gram-negative bacteria. Furthermore, nanowire topographies inspired by cicada wings have been demonstrated to be quite effective, particularly against Gram-negative bacteria [26].

### 1.3.3 Electrochemical Deposition

Electrochemical deposition (ECD) is a highly effective method that involves the precise movement of charged particles or polymer macromolecules towards an electrode under the influence of an electric field, ensuring optimal results.

Nanoparticles such as Ag, Cu, and ZnO have been successfully utilized in treating implant-related infections in recent years. To enhance biocompatibility, nanoparticles are frequently combined with polymers, such as chitosan, which is synthesized by deacetylation of chitin, the second most abundant natural polysaccharide. The materials occur naturally and have a biocompatible structure similar to that of hyaluronic acid and glycosaminoglycan extracellular matrix molecules. Chitosan coating techniques include solution casting, layer-by-layer deposition, and electrochemical deposition [30]. Electrochemical deposition enables the production of tunable and homogeneous coatings, making it an attractive method for chitosan and chitosan-based coatings. This has resulted in a recent surge of interest in this field[31].

HA was used to promote bone osteogenesis, while Ag and chitosan were incorporated to provide antibacterial properties. Pulsed electrodeposition was employed, resulting in a significant increase in surface coating efficiency when the speed was controlled[30] .

Coating the implant surface with nanotube structures is a preferable solution to overcome limitations with implants. This is due to the fact that tissues are more likely to encounter a biocompatible material such as nanotubes, rather than a hard structure such as an implant, which can decrease the likelihood of implant failures. Graphene, with its two-dimensional nanostructures, is commonly used in many fields and can be preferred for its anti-bacterial effect. It is important to note that increasing amounts of graphene may have toxic effects. To determine the optimal surface dosage, we utilized the electrochemical deposition method and continued the process until bacterial inhibition was achieved without causing toxicity [32].

ECD possesses several advantages over other techniques. These include low costs, high product purity, high deposition rates, homogeneous coating distribution, the ability to combine different monomers to obtain copolymers with a wide range of compositions (e.g. electropolymerisation), the possibility of using complex substrate geometries, waste reduction, ease of process control and automation. By controlling the ECD operating conditions, such as initial pH, electrolytic solution composition, current density, deposition time and temperature, electrochemical cell typology or experimental design, it is possible to obtain polymer coatings with customised

morphology and assemblies in a simple manner. These outstanding issues represent current research challenges that need to be addressed. Electropolymerisation and electrodeposition typically result in the formation of a dense polymer. However, the growth of a passivating polymer film inhibits further polymer deposition (in electrodeposition) or monomer migration (in electropolymerisation) on the electrode surface, resulting in only very thin coatings. To create highly porous structures or to achieve thick coatings on titanium, additional techniques must be employed [33].

### 1.3.4 Electrophoretic Deposition

Electrophoretic deposition (EPD) is the preferred method for depositing inorganic particles, biopolymers, and hybrid combinations of both. EPD is based on the movement of charged particles or molecules in a liquid medium by the action of direct current applied between two electrodes. It offers numerous advantages such as low cost, short processing time, and simple installation. Additionally, it can be used to coat complex shapes with ease. The process is highly versatile and can be used for the processing of biological molecules and drugs, as it can be carried out at room temperature. It is capable of depositing particles of various sizes, ranging from nanometres to microns, as well as for deposition on substrates and multilayer coatings with large surface areas. Consistent coatings can be easily created by adjusting the deposition voltage, time, and inter-electrode distance, or by modifying the suspension properties such as concentration, pH, and stability. This allows for precise control of coating thickness and the amount of antimicrobial deposited [34, 35].

Similarly, HA, which has biocompatibility and bioactive qualities similar to bone structure, is recommended as a coating material. Cu ions have been proposed as an antibacterial agent. Cu ions, which are also present in metabolic fractions, provide antibacterial activity in three ways. The first is the binding of metal ions to proteins, which neutralizes bacteria; the second is metal ions passing through the microorganism membrane, which causes structural changes in bacteria; and the third is metal ions interacting with microbial nucleic acid, which prevents bacteria from multiplying. Oct is the accumulation of suspended particles charged by

electrophoretic forces on the electrodes, in addition to the benefits of EPD, and the manufacture of appropriate coatings [36].

Different antimicrobial coatings in EPD coatings have been studied. For example, release-killing antibacterial coatings are classified as organic or inorganic. First, there are organic antibacterial coatings. It includes broad-spectrum antibiotics like gentamicin, vancomycin, and levofloxacin, as well as phytotherapeutics like curcumin and ferulic acid that do not cause drug resistance, or carrier systems like titania nanotubes, mesoporous silica-based nanoparticles, polymer particles, and magnetic nanoparticles that are used to extend drug release time. Inorganic antibacterials are metallic nanoparticles, bioactive glasses, carbon nanotubes, graphene oxide and others. Cationic substances (quaternary ammonium compounds (QACs), chitosan, antimicrobial cationic peptides (AMPs), etc.) or antimicrobial enzymes (AMEs) are used to make contact-killing coatings [34].

### 1.3.5 Sol–gel Coating

The sol-gel technique is a low-temperature wet chemical approach for generating inorganic or biologically modified glass and ceramic oxides. The creation of sol, a stable colloidal suspension of small nanosized particles in aqueous or alcohol solution, is the first step in the procedure. Hydrolysis and partial condensation of inorganic metal salts or metal-organic compounds, primarily metal alkoxides, yields sol. These sol precursor chemicals are often dissolved in an alcohol-water solution, where water hydrolyzes them. Alcohol is frequently used as a homogenizer. Condensation reactions begin once the hydrolysis products are generated, and the two events might occur concurrently. The persistence of condensation processes and particle aggregation within the sol results in the creation of a 3D network that holds leftover solvents and water. With increasing viscosity, the transition from sol to gel becomes obvious. Water or other solutes are removed from the gel as it forms, causing observable changes in the gel.

Various synthesis parameters influence the rate and degree of hydrolysis-condensation, which in turn affect the final material's characteristics. The choice of precursor, for instance, influences the degree of oligomerization or polymerization through the hydrolysis and condensation reaction, thereby affecting the end product.

Additionally, the relative rate of hydrolysis-condensation processes is affected by the use of acid or base catalysts, which is determined by the pH. Reactions proceed slowly in a neutral environment, while unreacted products are present in an acidic environment, and severe branching gelation occurs in a basic environment. The ratio of precursor water or solvents has little influence on the reactions. Temperature does not affect reaction speed, but it does influence the evaporation of water and solvents during the drying stages [1].

Highly porous, nanostructured controlled release materials processed using silica sol-gels at room temperature have been extensively studied. These materials are renowned for their unique properties[37]. The implant surfaces were made biocompatible by coating them with a TiO<sub>2</sub> sol-gel [38]. The antibiotic combination was confidently coated with HA using the sol-gel method to achieve strong antibacterial properties [39].

#### 1.3.5.1 Spray-Coating

The sol-gel method can be combined with spray coating to deposit fine droplets of the sol onto the substrate using a nozzle system. To achieve nebulisation, the sol viscosity must be lower than that of the dip and spin coating technique. Coalescence of fine droplets can occur if the surface is wettable. This technique is widely used in industrial applications due to its speed and suitability for irregularly shaped substrates, as well as its low waste of coating sol. It is important to note that the system tip may become clogged over time due to solvent evaporation and resulting sol gelation. However, this challenge can be overcome by implementing proper maintenance procedures. Furthermore, coating hydrophobic surfaces can be challenging, but with the right techniques and expertise, it can be achieved successfully [1]. The spray coating used for implants and prostheses ranges from 30 to 100 microns in thickness, promoting bone growth and adhesion [40]

#### 1.3.5.2 Spin-coating

In spin coating, drops of sol are dispersed onto the substrate surface and the substrate is then spun at high speed. Sol viscosity, rotation speed and surface tension are the

parameters that control the thickness and uniformity of the film. In general, spin coating is preferred for flat surfaces [40].

Spin coating is a low cost process that can produce thin films with consistent properties and has potential for process scale-up. Although generally preferred for flat surfaces, it can be used with other coating types to create three-dimensional frameworks. In addition, spin coating has been preferred to develop coatings using simple systems or glass microparticle suspensions [41].

### 1.3.5.3 Dip-coating

Sol-gel dip coating is a highly effective and straightforward technique used in coating technologies to coat the surface of regular materials. The process involves three simple steps: dipping, residence, and withdrawal. Adhesion of the coating to the substrate is a critical factor to consider in coatings. However, sol-gel dip coating has successfully overcome this limitation, ensuring that coating properties are not lost and living tissue is not damaged [4, 42].

Sol-gel dip coating has numerous advantages, such as high purity and homogeneity, low processing temperatures, reduced thickness, and easy and inexpensive preparation methods [43]. By incorporating organic components into the inorganic sol, the limitations of inorganic sol-gel coatings, such as brittleness and relatively high processing temperatures, can be overcome. This leads to the production of organic-inorganic nanocomposite materials at low processing temperatures. The molecular-level bonding of the two-phase materials enables homogeneity and the formation of materials that exhibit a synergetic effect when combined. Two types of hybrids can be obtained: Class I hybrids, characterized by weak bonds between the two phases (such as hydrogen bonds and Van der Waals forces), and Class II hybrids, in which the components interact with strong bonds (such as covalent or ionic-covalent bonds). The properties of materials, including thermal behaviour, mechanical properties, stability and solution dispersion, are affected by the nature of the bonds between the organic and inorganic phases [44].

For the dip coating method, PVA polymers with a unique solution matrix and excellent adhesion properties, film formation, high tensile strength, and flexibility are the preferred choice [45]. PVA polymer is biocompatible and safe, as observed in animal experiments, due to its inert and stable nature. Its unique properties such as adhesion, durability, film formation, swelling, and security make it a popular choice in various areas, including biomedical applications. The properties of PVA are determined by various factors such as the preparation method, molecular weight, arrangement in the polymer chain, degree of polymerization, and degree of hydrolysis. By controlling these factors, the desired properties can be achieved [46]. Furthermore, when PVA is combined with antibacterial materials, it exhibits antimicrobial properties without requiring any active substance as a binder [47].

The surface of Ti alloy implants is treated with the compound that utilizes direct covalent bonding of amphiphilic QAS, without the need for auxiliary linkers [48]. Compound quaternary ammonium compounds were the preferred disinfectants for uninjured skin surfaces, non-seriously damaged surfaces, and mucous membranes in the study. SiQAC's hydrolysis products also demonstrated antimicrobial properties against a wide range of microorganisms while chemically interacting with different surfaces. QASs contribute to bacterial inhibition by negatively affecting the cell wall and positively affecting this function [49]. The compound's antimicrobial activity is due to its lengthy, lipophilic -C18 H37 alkyl chain, which permeates bacterial cell membranes, resulting in autolysis and bacterial cell death upon direct contact [50]. Alkoxysilane-based QACs can be easily attached to various materials containing OH groups, such as glass, titanium, cellulose, silicon, and PVA, as well as other materials like polymers and metals, after a preparation process. The strong triple Si-O covalent bond significantly enhances the solution's stability across a wide range of pH and temperature. Antimicrobial properties can be achieved without the need for any active substance as a binder when PVA and QAS are used together [47]. Because of these properties and their low toxicity, quaternary ammonium silanes (QAS) may be preferred as a material to help overcome post-implant infections and provide bactericidal properties [50].

# Chapter 2

## 2. Materials and Methods

### 2.1 Preparation of Coating Solutions

#### 2.1.1 Preparation of Polyvinyl Alcohol (PVA) Phase

The concentration of PVA was confidently adjusted to 5%. Absolute ethanol, which acts as a cosolvent, was added to the solution in the same ratio as tetraethyl orthosilicate TEOS ( $M_w 208 \text{ g mol}^{-1}$ ) before adding the left part. Silica sol was expertly produced by partially hydrolysing TEOS in acidified water using nitric acid ( $\text{HNO}_3$ ) as a catalyst, with a precise TEOS/ $\text{H}_2\text{O}$ / $\text{HNO}_3$  volume ratio of 1/1/0.1. The mixture was confidently stirred until a clear solution was obtained [51]. After clarification, the pH was measured and it was observed that the hydrolysis reaction occurred at pH 2. NaOH was then added to the mixture to bring the pH to 7, allowing the condensation reaction to occur [50]. To achieve a coatable consistency for the sol gel, we conducted brewings using different TEOS: WATER v/v ratios, specifically 1:6, 1:12, 1:18, and 1:24.

#### 2.1.2 Mixing of Silane Content with PVA Solution

The concentration of PVA was confidently adjusted to 5%. Absolute ethanol, which acts as a cosolvent, was added to the solution in the same ratio as TEOS before adding the left part. Silica sol was expertly produced by partially hydrolysing (TEOS) in acidified water using nitric acid ( $\text{HNO}_3$ ) as a catalyst, with a precise TEOS/ $\text{H}_2\text{O}$ / $\text{HNO}_3$  volume ratio of 1/1/0.1. The mixture was confidently stirred until a clear solution was obtained[51]. The Dimethyloctadecyl[3-(trimethoxysilyl)propyl]ammonium chloride solution ( $M_w 496.28 \text{ g mol}^{-1}$ ) and TEOS ( $M_w 208 \text{ g mol}^{-1}$ ) were combined in a 1:1 mol ratio and added to the QAS

solution while keeping the silanol constant in volume [49, 52]. After clarification, the pH was measured and it was observed that the hydrolysis reaction occurred at pH 2. NaOH was then added to the mixture to bring the pH to 7, allowing the condensation reaction to occur [50].

## 2.2 Dip Coating Process

When using the dip coating method, it is important to carry out each step with care. For instance, it is crucial to wait for the part to become fully wet and for the necessary chemical processes to take place. Additionally, the substrate should be pulled vertically through the liquid at a controlled speed, temperature, and pressure. Environmental conditions, such as solution chemicals, temperature, and humidity, can affect the film thickness and the mentioned processes [53]. The dip coating process tested dipping speeds of 100, 60, 50, and 40 mm/min, with waiting times of 30, 60, 80, and 99 seconds for the surface in the solution. To optimize coating thickness, the second and third coats were applied either immediately on top of the first coat or after it had dried, in one, two, or three coats.

## 2.3 Characterization of Dip Coated Surfaces

The coating solution and coated surface underwent physicochemical characterization using methods such as contact angle, SEM, surface cation density, Raman and rheological analysis. Further details are provided in the following sections.

### 2.3.1 Rheological Analysis

Non-Newtonian and Newtonian properties of the coating solution were analyzed with the Hybrid Rheometer Discovery HR-2 Device to evaluate. Rheological analysis studies are carried out to evaluate the surface coating capability of the coating solutions prepared.

### 2.3.2 Scanning Electron Microscope (SEM) Analysis

SEM analysis was performed to investigate the thickness and evenness of the coating layers. For this purpose; The slides coated with a dip were observed using a scanning electron microscope (SEM) (Carl Zeiss 300VP, Germany) operated at 5 kV. To reduce the sample arc size during SEM observation, a thin layer of gold was coated on the glass slide surface using an automatic sputter coater (Emitech K550X). For this analysis, coatings were prepared and analyzed using SEM.

### 2.3.3 Surface Cation Density ( $\text{NH}_4/\text{cm}^2$ ) Analysis

Surface cation density is important for providing bactericidal activity through electrostatic interaction with bacteria that have a negative surface charge. For this purpose, we investigated surface cation density values. The cationic charge density of the sample surfaces was determined by means of fluorescent staining. Circular coupons with a diameter of 12 mm were coated and immersed in 2 mL of 1% fluorescein (disodium salt) solution in demineralised water. The samples were then shaken at 60 rpm for 10 minutes. After that, the samples were washed three times with 2 mL of demineralised water to remove any dye that did not complex with cationic charges. The samples were placed in 2 mL of a 0.1 wt% solution of cetyltrimethylammonium bromide in distilled water and sonicated for 5 minutes. They were then shaken at 60 rpm for 5 minutes to desorb the complex fluorescent dye. 200 mL of 100 mM phosphate buffer (pH 8) was added, followed by measuring fluorescence using a T70+ UV/VIS Spectrometer at a wavelength of 501 nm. This process was repeated three times to ensure accuracy. The formula used to estimate surface cationic density is as follows:

$$DYE = \frac{ABS}{\epsilon \times L} \quad (2.1)$$

$$\text{Charge Density} = \frac{DYE \times V \times N}{A} \quad (2.2)$$

ABS is the fluorescein optical density at 501 nm,  $V$ : is the volume,  $L$  is the length of a polystyrene cuvet(1 cm),  $N$ : Avogadro number ( $6.023 \times 10^{23} \text{ mol}^{-1}$ ),  $V$  is the volume of the extraction solution (1,5 mL),  $A$  is the surface area of the sample and  $\epsilon$ : fluorescein molar absorptivity or molar extinction coefficient ( $77 \text{ L mM}^{-1} \text{ cm}^{-1}$ ) [54, 55].

### 2.3.4 Contact Angle

Hydrophobicity and hydrophilicity analysis was conducted on the coated surfaces using the Attension Theta device, which has a contact angle measurement range of  $0^\circ$ - $180^\circ$  and an accuracy of  $\pm 0.1^\circ$ . The contact angle analysis is provided results on the hydrophilicity and hydrophobicity of the coated surfaces. These results are used to evaluate the adhesion of bacteria to the surface or cell profiling [56].

### 2.3.5 Raman Spectrometry Analysis

Raman scattering is the result of inelastic scattering caused by the vibration of bonded atoms in a molecule or crystal lattice when exposed to a powerful laser source. The Renishaw Raman Spectrometer interacts with the incoming beam to produce this effect. The peaks in the spectrum obtained from scatterings can provide information about the functional groups that make up the structure of the material, as well as qualitative and quantitative analysis of the material. This is achieved by examining the bond structures of organic or inorganic substances in the sample. The samples prepared for coating were taken to the Raman spectrophotometer for bonding structure analysis. The coating solution composed of the formed of Si-O-Si bonds through the pH effect is examined [49, 52, 57]. It also detects the presence of  $\text{NH}_4$ , which provides antibacterial activity was also evaluated in order to solid the potency of antibacterial activity of the coating layers.

## 2.4 *In vitro* Studies and Cytotoxicity Studies

### 2.4.1 *In vitro* Antibacterial Studies

The study employed Gram-positive *S. aureus* ATCC 29213. The bacteria were distributed on agar plates and incubated at 37°C overnight after being taken from frozen stocks stored at -80°C. Following overnight incubation on tryptic soy agar (TSA), a single colony was selected and transferred to 5 mL of tryptic soy broth (TSB). The culture solution was incubated overnight at 37°C on an orbital shaker (180 RPM). After 18 hours, the refresh process was performed by adding 200 µl of post-incubation bacterial solution to 5 ml of TSB. The mixture was then left to incubate for an additional 2 hours at 37°C and 180 RPM. Following this, 100 microliters of clean TSB and 100 microliters of bacterial solution were added to the 96-well plate. OD adjustment was performed at a wavelength of 600 nm on the BioTek Synergy HTX multi-mode reader device. The bacterial stock was adjusted to 10<sup>8</sup> CFU/ml.

#### 2.4.1.1 Investigating the Bacterial Cell Adhesion on K- Wire

PVA-TEOS-QAS was tested for its antibacterial potential against *S. aureus* ATCC 29213 using TSB and TSA as liquid and solid growth media, respectively. The Alamar Blue Assay was performed using ready-to-use Resazurin (R&D Systems, USA). Bacteria were adjusted to a concentration of 10<sup>5</sup> CFU/mL in test tubes. K-wires, adjusted to 1.5 cm in length, were incubated for 6 hours at 37 °C in 2.5 ml of bacterial solutions. After the incubation period, 100 microliters were transferred into 96-well plates. Then, 10 µL of ready-to-use resazurin (R&D Systems, USA) was added to each well. The plates were incubated with resazurin for 2-4 hours, and fluorescence intensity was measured at excitation values of 540 and emission of 600 using the BioTek Synergy HTX multi-mode plate reader. Bacterial solutions were serially diluted and colony counts were determined on agar plates.

In the next stage, the K-wires removed from the bacterial solution were washed three times with PBS. Then, PBS was added to the K-wires and sonication for 30 seconds, followed by vortexing for 30 seconds. This process was repeated three times to ensure that the bacteria adhering to the K-wire were in PBS. Subsequently, 100

microliters of the solution were transferred into a 96-well plate, and 10  $\mu\text{L}$  of ready-to-use resazurin (R&D Systems, USA) was added to each well. After incubating with resazurin for 2-4 hours, fluorescence intensity was measured using the BioTek Synergy HTX multi-mode plate reader with excitation values of 540 and emission of 600. Colony counting was performed on the agar plate through serial dilution, following the same process as before.

After sonication and vortexing, 100  $\mu\text{l}$  of the solution was taken and incubated in a clean TSB environment at 37°C and 180 rpm for 18 hours. The aim of this experiment was to determine whether the bacteria adhering to the K-wire could be recultured. After 18 hours of incubation, 100 microliters of the sample were transferred into 96-well plates. Then, 10  $\mu\text{L}$  of ready-to-use resazurin (R&D Systems, USA) was added to each well. The fluorescence intensity was measured at excitation values of 540 and emission of 600 using the BioTek Synergy HTX multi-mode plate reader after 2-4 hours of incubation with resazurin.

#### 2.4.1.2 Investigation of *In vitro* Antibiofilm Effect

The antibiofilm potential of PVA-TEOS-QAS against *S. aureus* ATCC 29213 is evaluated for effectiveness. The starting bacterial culture for biofilm development was  $10^5$  CFU/mL of the diluted bacterial culture. To promote biofilm development, 0.2% (w/v) glucose was added to the culture. Next, 500  $\mu\text{L}$  of the prepared bacterial solution was placed in each well of the 24-well plate, and 1.5 cm long K-Wires were placed on the flat bottom of the plate. The plate was then placed on an orbital shaker for 24 hours at 37°C and 180 rpm.

This study investigates the prevention of *S. aureus* bacterial biofilm formation on K-Wire coated with PVA-TEOS-QAS. K-Wires were incubated for 24 hours to form *S. aureus* biofilms. After incubation, the biofilms were washed with PBS to remove loosely attached bacteria. A resazurin assay was performed by adding 10% Alamar Blue solution to the total PBS volume. The fluorescence intensity was determined using HTX multi-mode rendering, with measurements taken at 540 excitation and 600 emission. Following the resazurin analysis, crystal violet analysis was conducted. To do this, the wells were washed and dried before incubating 200  $\mu\text{L}$  of 2.3% w/v crystal violet solution at room temperature for 5 minutes. The stain was

then removed, and the wells were washed twice with distilled water. The biofilms were diluted in 200  $\mu\text{L}$  of 96% ethanol. The plates were then incubated at room temperature for 1 hour. After incubation, 100  $\mu\text{L}$  of each sample was taken for spectroscopy examinations. The absorbance was measured at 595 nm to assess biofilm mass and viability, with an untreated biofilm control used as a reference [58].

### 2.4.2 *In Vitro* Cytocompatibility Investigations

Noncoated wire, PVA-TEOS and PVA-TEOS-QAS is evaluated in terms of biocompatibility. To this end; UV-sterilized coated K-Wire were immersed in 5 mL Dulbecco's modified Eagle medium (DMEM; Sigma Aldrich) supplemented with 10% fetal bovine serum (FBS; Sigma Aldrich) and 1% penicillin–streptomycin (10,000 units/mL penicillin, 10,000  $\text{lg}/\text{mL}$  streptomycin) for 24 h in a cell culture incubator at  $37^{\circ}\text{C}$  under 5%  $\text{CO}_2$  to extract the reservoir for cytotoxicity investigations. Cytotoxicity studies were conducted following ISO 10993-5 standards. A volume of 635 microliters of cell medium with a concentration of  $125 \text{ mm}^2/\text{ml}^{-1}$  was added onto a 1.5 cm K-Wire. The K-Wire was then incubated at  $37^{\circ}\text{C}$  under 5%  $\text{CO}_2$  for 24 hours while being shaken at 180 rpm [59].

*In vitro* cytotoxicity tests are performed on L929 rat fibroblast cells. The L929 cell lines are cultured in DMEM, which contains 4500 mg/L glucose, L-glutamine, sodium pyruvate, and sodium bicarbonate. This medium is sterile filtered and suitable for cell culture, as described on the company website. Additionally, the DMEM medium is supplemented with 10% fetal bovine serum (FBS) and 1% penicillin-streptomycin before being added to the cells.

The cells are incubated in a cell incubator at  $37^{\circ}\text{C}$  under 5%  $\text{CO}_2$  with high relative humidity (90 to 95%). The cell culture medium is refreshed every two days. Once the cell density reaches 80%, they are treated with trypsin and then seeded into 96-well plates at a concentration of  $10^4$  cells per well. The cells are incubated overnight to attach to surfaces. The extracted samples is then be added to cells at rates of 100%, 50%, and 25%, following ISO 10993-5 standards [59]. The cells are incubated for 24 hours at  $37^{\circ}\text{C}$  under 5%  $\text{CO}_2$ . Afterward, 10  $\mu\text{L}$  of ready-to-use resazurin (R&D Systems, USA) is added to each well.

The fluorescence intensity is measured at excitation values of 540 and emission values of 600 using the BioTek Synergy HTX multi-mode plate reader after 2-4 hours of incubation with resazurin.



# Chapter 3

## 3. Result and Discussion

### 3.1 Characterization of Coating Surfaces

#### 3.1.1 Rheological Analysis

A review of the literature shows that the dip coating process behaviour of Newtonian fluids has been investigated using various models. In these studies, the required thickness values were also achieved with Newtonian fluids [56]. The rheological analysis of two different liquids, PVA-TEOS and PVA-TEOS-QAS, was conducted in the experiments. Both liquids were found to be fluid. Figure 3.1 shows the stress and viscosity curves of PVA-TEOS, which exhibits two Newtonian types. Similarly, Figure 3.2 shows the stress and viscosity curves of PVA-TEOS-QAS.

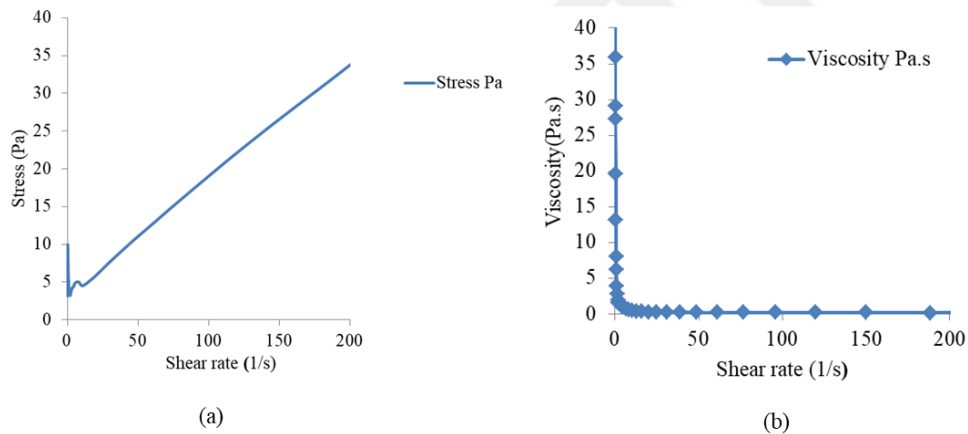


Figure 3. 1: Rheological analysis of (a) Stress Curve and (b) Viscosity Curve of PVA-TEOS, where condensation reactions take place

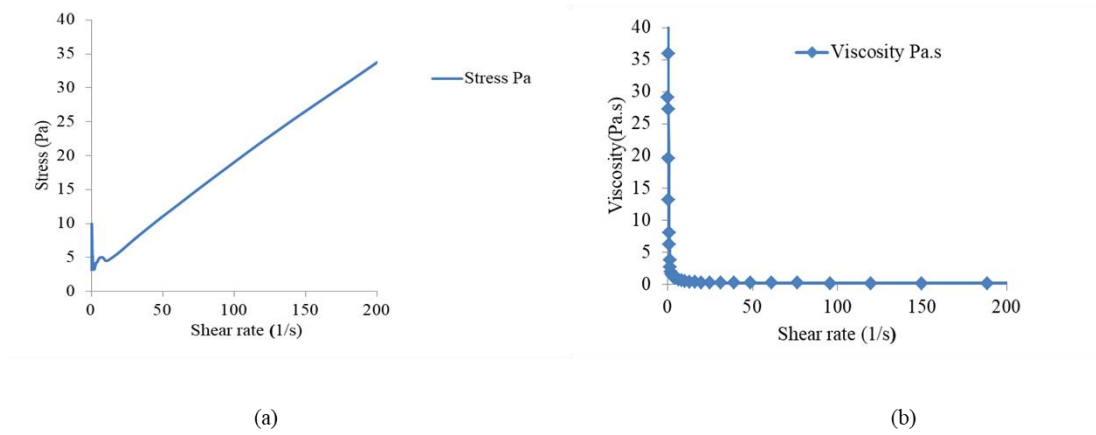


Figure 3. 2: Rheological analysis of (a) Stress Curve and (b) Viscosity Curve of PVA-TEOS-QAS, where condensation reactions take place

### 3.1.2 Scanning Electron Microscope (SEM) Analysis

According to the literature, achieving a crack-free and homogeneous surface coating is crucial when using the sol-gel dip coating method [43, 59, 60]. Figure 3.3 shows that the coatings were initially applied in a single layer at a speed of 100 mm/min for 30 seconds, followed by a waiting time of 60 seconds. Alternatively, they were applied in three layers without waiting for drying. Cracks were observed on the surface of both coatings, regardless of the waiting time for single-layer coatings at a speed of 100 mm/min. In three-coat coatings at the same speed, a deep crack appeared on the coating surface with a waiting time of 30 seconds. The waiting time of 60 seconds is relatively better in both coating types.

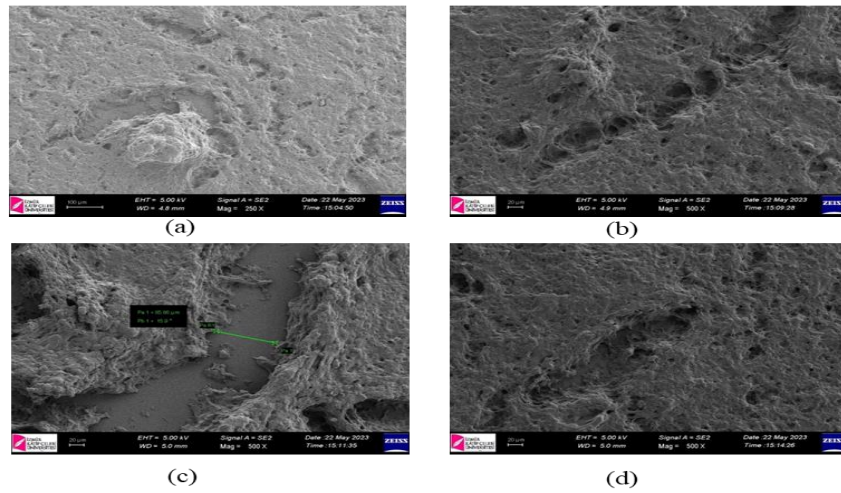


Figure 3. 3: SEM analysis of (a) 100 mm/min 1x 30sec, (b) 100 mm/min 1x 60 sec, (c) 100 mm/min 3x 30 sec (d) 100 mm/min 3x 60 sec of glass lam surface coatings performed at different drawing speeds, single layer and triple layer and different waiting times

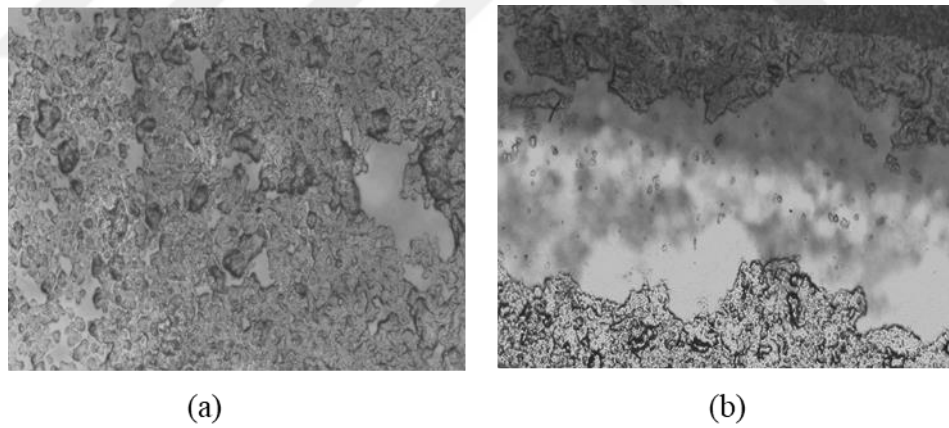


Figure 3. 4: Light microscope image of the coatings applied on the glass lam surface  
a) 40 mm/min 1x 60sec, (b) 100-80 mm/min 2x 30-60 sec

It was found that the drawing speed had a negative impact on the surface coating, resulting in gaps even when observed under a light microscope at a speed of 40 mm/min, as shown in Figure 3.4 (a). To prevent cracks in the 3-layer coating, a second layer of coating was applied after allowing the first layer to dry. However, it was observed that the dried surface separated from the surface with the second layer of coating, as depicted in Figure 3.4 (b).

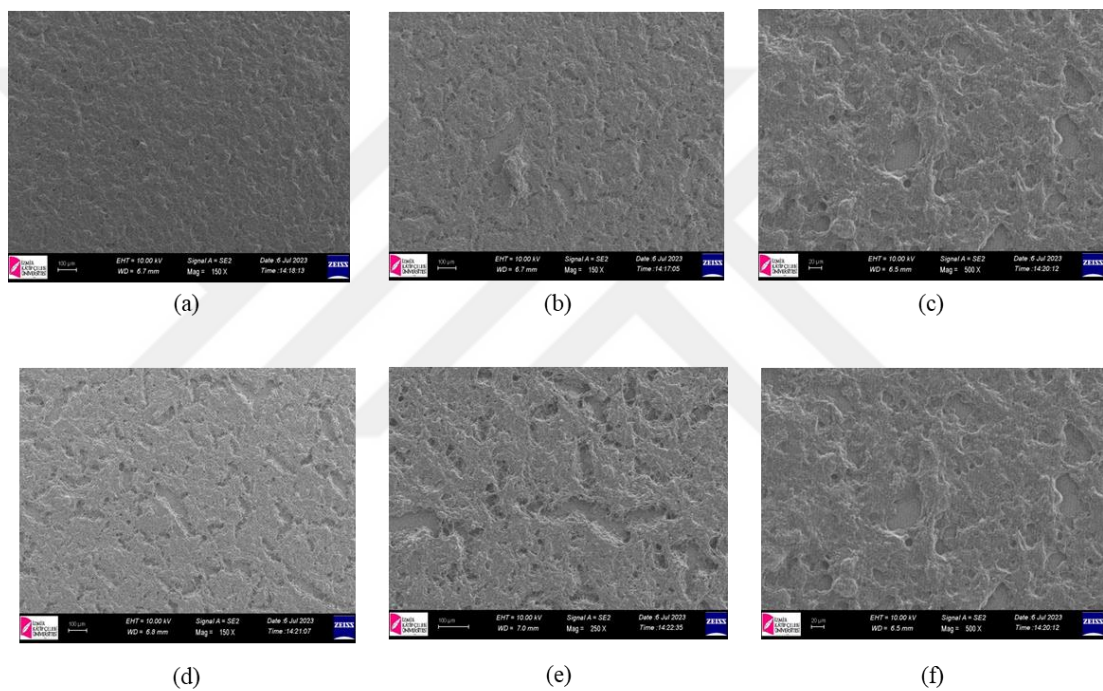


Figure 3. 5: SEM analysis of PVA-TEOS coatings applied on glass lam surface in one layer and two layers at different waiting times at a constant speed (a) 50 mm/min 1x 60 sec, (b) 50 mm/min 1x 80 sec, (c) 50 mm/min. min 1x 99 sec (d) 50 mm/min 2x 60 sec (e) 50 mm/min 2x 80 sec, (f) 50 mm/min 2x 99 sec

Following the dip coating process, we conducted single and two-coat coatings at waiting times of 60, 80, and 99 seconds, as shown in Figure 3.5 Our aim was to optimize the waiting time and number of layers, with the ideal speed being 50

mm/min. We were able to obtain flawless and homogeneous coatings with a speed of 50 mm/min, a dwell time of 60 seconds and a single layer.

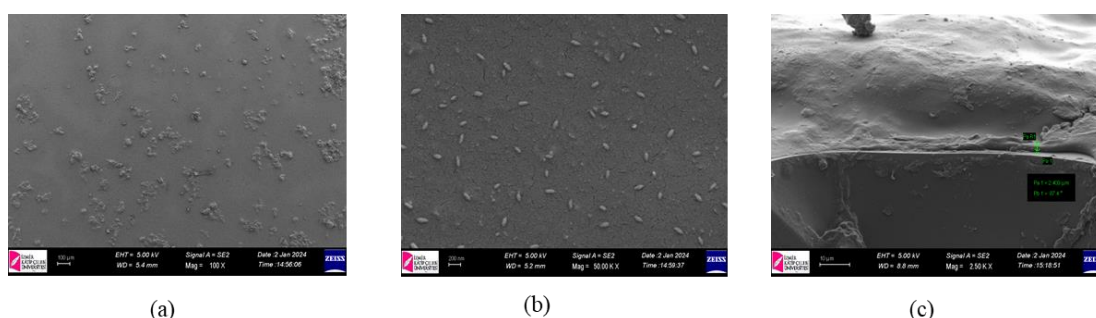


Figure 3. 6: SEM images of the determination of the surface topology and thickness of the coatings applied to the glass lam surface (a) PVA-TEOS, (b) PVA-TEOS-QAS, (c) PVA-TEOS-QAS T

The coatings of PVA-TEOS and PVA-TEOS-QAS were applied according to the procedure illustrated in Figure 3.6. A single coat was applied at a speed of 50 mm/min, followed by a waiting time of 60 seconds. The coating solution was optimised using PVA-TEOS, and the resulting coating thickness was measured at 2,409 micrometers in Figure 3.6 (c).

### 3.1.3 Surface Cation Density ( $\text{NH}_4/\text{cm}^2$ ) Analysis

The calculation of surface cationic density was performed on a single layer coating applied to a 12 mm diameter glass coupon. The coating was applied at a speed of 50 mm/min and left to settle for 60 seconds. The literature states that the absorbance value corresponding to quaternary ammonium compounds that can form an ionic complex with negatively charged ammonium molecules was measured. Calculations were carried out as described, and the resulting value was  $69.68 \times 10^{17}$  mmol/  $\text{cm}^2$ . This value is significantly higher than the  $10^{14}$  charge per  $\text{cm}^2$  required to kill bacteria upon contact [55, 61, 62].

### 3.1.4 Contact Angle

The literature suggests that modifying the surface hydrophobicity or hydrophilicity of biomaterials can prevent bacterial adhesion and enhance biocompatibility. High surface compliance is expected for implant tissue cells [63–65]. Hydrophilic coatings can enhance the success of implants by supporting cell profiles. Figure 3.7 shows the recorded values of  $46,1^\circ$  for glass lamellae,  $64,4^\circ$  for PVA-TEOS, and  $78,4^\circ$  for PVA-TEOS-QAS.

Although the coating material causes a decrease in hydrophilicity, the values still indicate hydrophilic properties, which can support cell proliferation on coated implant surfaces.

In the literature, studies have been conducted on the binding of *S. aureus* to hydrophilic and hydrophobic surfaces. The study found that *S. aureus* interacted with both types of surfaces. Changing surface hydrophobicity during contact angle measurement is an indication that its effectiveness in terms of bactericidal activity has not changed[66].

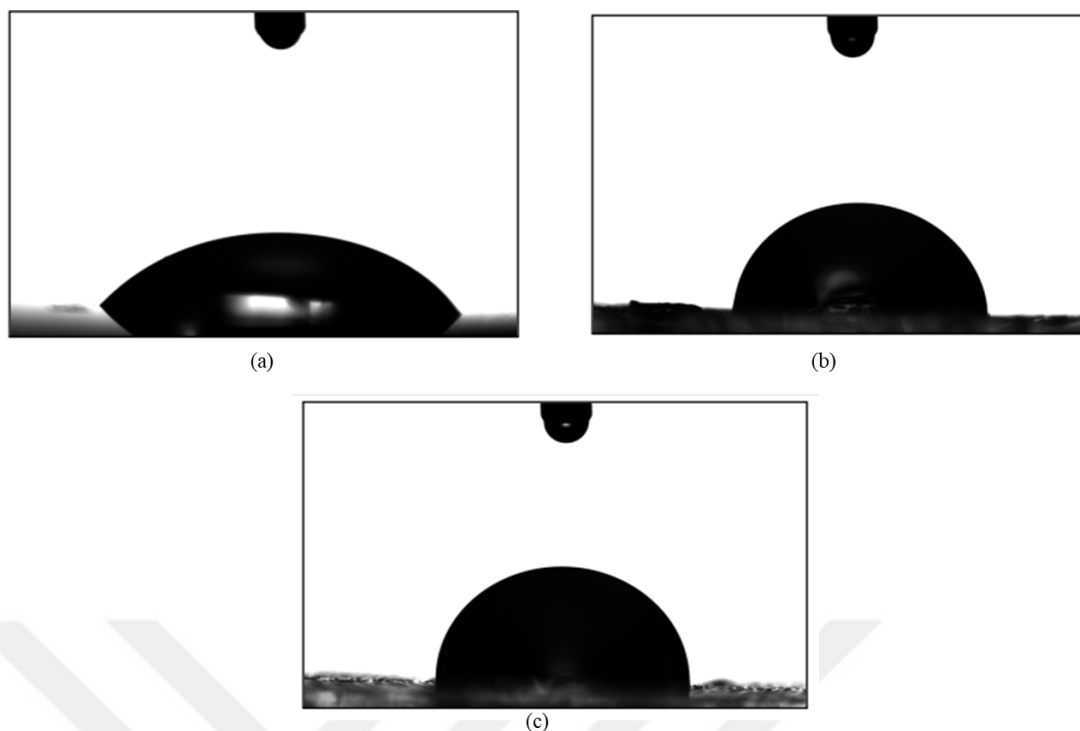


Figure 3. 7: Contact angle measurement of the coated surface and samples made with coating solutions (a) Glass, (b) PVA-TEOS, (c) PVA-TEOS-QAS

### 3.1.5 Raman Spectrometry Analysis

Figure 3.7 (a) shows the Raman data for PVA-TEOS-QAS at pH 2 and pH 7. The condensation reaction was pH-dependent. The peak at  $1100\text{ cm}^{-1}$  indicates the formation of the Si-O-Si bond, consistent with literature. The sol-gel formation was completed [52, 57].

Figure 3.8 (b) shows the Raman data for PVA-TEOS and PVA-TEOS-QAS at equal pH values. The presence of cations on the surface is crucial for providing antibacterial properties. According to the literature, the peak values at  $1300\text{ cm}^{-1}$  indicate the presence of cations [67].

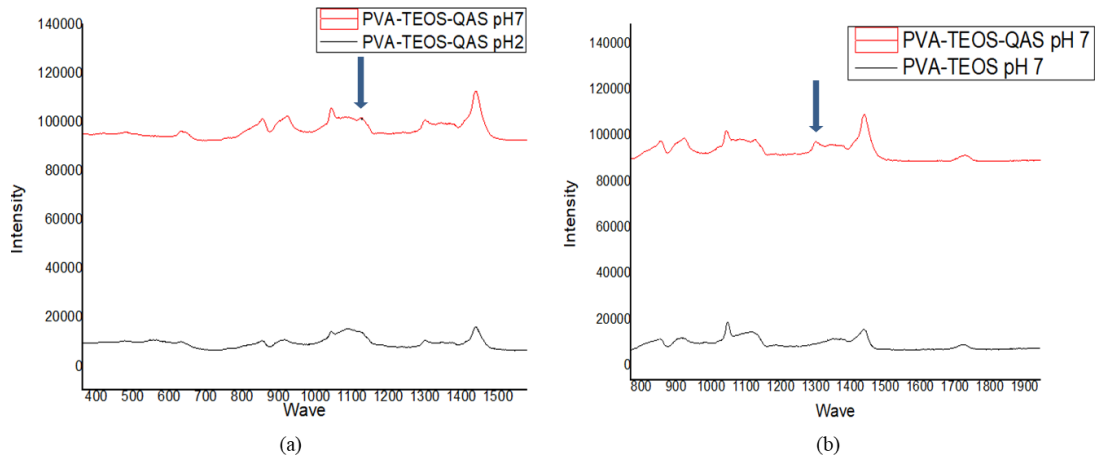


Figure 3. 8: Hydrolysis and condensation reactions were completed PVA-TEOS and incorporated into the coating matrix of QAS, and Raman Spectrometry analysis was performed (a) Si-O-Si Bond, (b) Ammonium Salts

## 3.2 *In vitro* Studies and Cytotoxicity Studies

### 3.2.1 Bacterial Cell Adhesion Research on K- Wire

Statistical analyses were performed using GraphPad Prism 8.4.2 One-way ANOVA and p value style: GP: 0,1234 (ns), 0,0332(\*), 0,0021(\*\*), 0,0002(\*\*\*), <0,0001(\*\*\*\*). In the graph in Figure 3.9, the efficacy on bacteria after 6 hours was determined by colony counting. However, as can be seen from the statistical analysis, no significant results were obtained by colony counting. There was no decrease in the bacterial LOG value. Literature studies have shown that K-Wires coated with PVA-TEOS-QAS exhibit bacteriostatic activity and cause a decrease of less than 1 LOG [68].

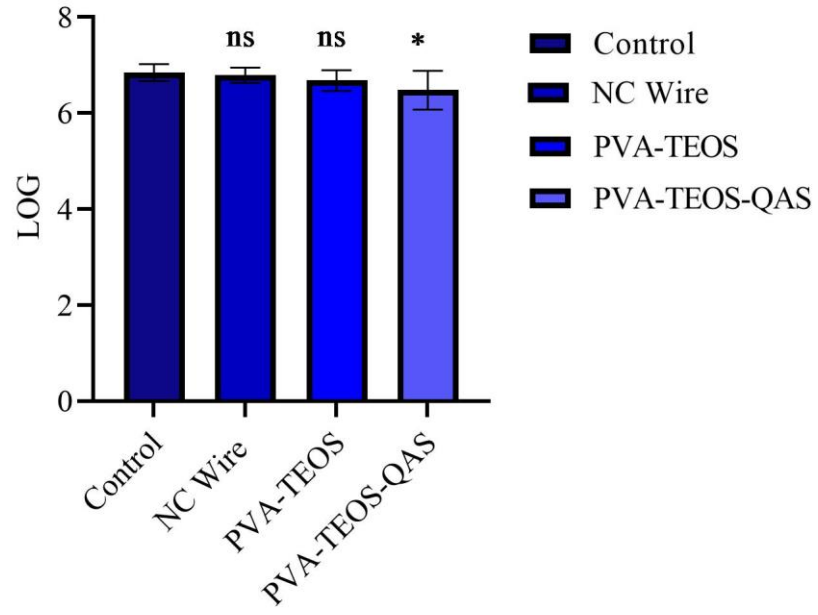


Figure 3. 9: Viability of *S. aureus* cells on K-Wires coated with as determined CTRL, NC Wire, PVA-TEOS, PVA-TEOS-QAS by coloni counting. (p value style: GP: 0,1234 (ns), 0,0332(\*), 0,0021(\*\*), 0,0002(\*\*\*), <0,0001(\*\*\*\*),One-way ANOVA)

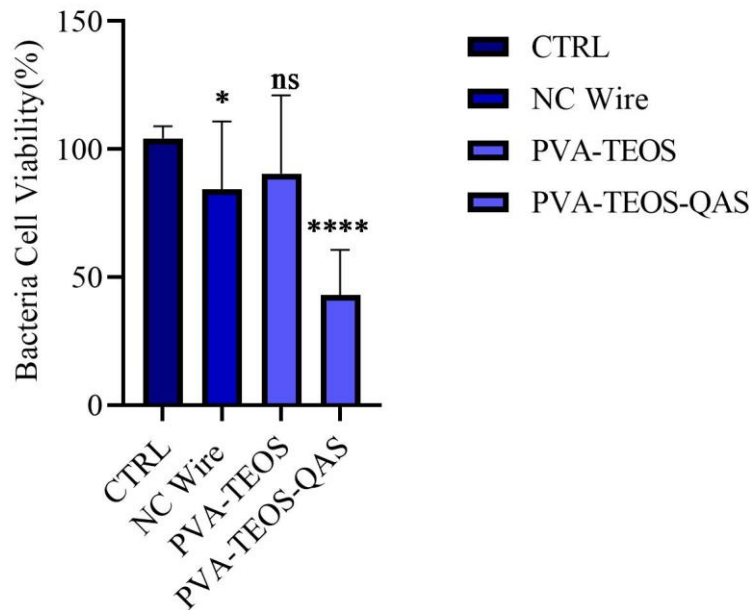


Figure 3. 10: Viability of *S. aureus* cells on K-Wires coated with as determined CTRL, NC Wire, PVA-TEOS, PVA-TEOS-QAS by Alamar blue assay. (p value style: GP: 0,1234 (ns), 0,0332(\*), 0,0021(\*\*), 0,0002(\*\*\*), <0,0001(\*\*\*\*), One-way ANOVA)

Statistical analyses were performed using GraphPad Prism 8.4.2. The experiments were repeated three times. One-way ANOVA was used to determine the p-values. The p-values were reported as follows: GP: 0.1234 (not significant), 0.0332 (\*), 0.0021 (\*\*), 0.0002 (\*\*\*) and <0.0001 (\*\*\*\*). Figure 3.10 shows the amount of *S. aureus* ATCC 29213 determined by the Alamar Blue assay in the bacterial solutions after 6 hours in the experiments repeated 3 times. The results indicate that PVA-TEOS and uncoated wires did not show a significant change compared to the control group. However, PVA-TEOS-QAS coated wires caused approximately 55% more deaths than the control groups.

Figure 3.11 shows colony counts after the K-wires were removed from the bacterial solution, washed three times, sonicated three times, and vortexed three times. The results indicate a reduction in LOG for PVA-TEOS-QAS coated K-Wires, suggesting a decrease in colonization potential. This is consistent with previous literature studies that have observed bactericidal activity for this coating. Simultaneously, the Alamar

Blue viability test was used due to its low bacterial adhesion detection limit, as shown in Figure 3.12. Upon examination of the figure and comparison with the control in Figure 3.10, it is evident that NC Wire, PVA-TEOS, and PVA-TEOS-QAS prevent bacterial adhesion. Additionally, bacterial activity was observed in K-Wires coated with PVA-TEOS-QAS[68].

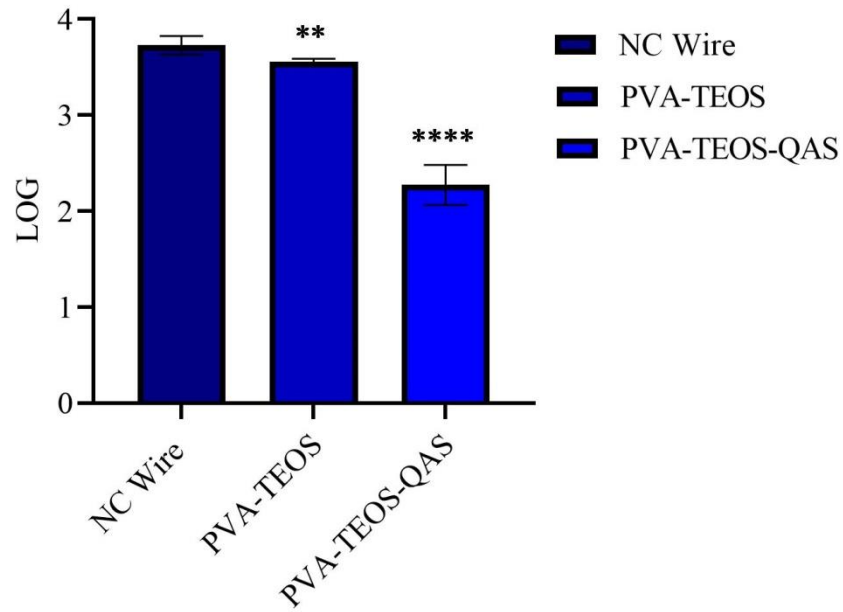


Figure 3. 11: Viability of adhered *S. aureus* cells on K-Wires coated with as determined NC Wire, PVA-TEOS, PVA-TEOS-QAS by coloni counting. (p value style: GP: 0,1234 (ns), 0,0332(\*), 0,0021(\*\*), 0,0002(\*\*\*), <0,0001(\*\*\*\*))

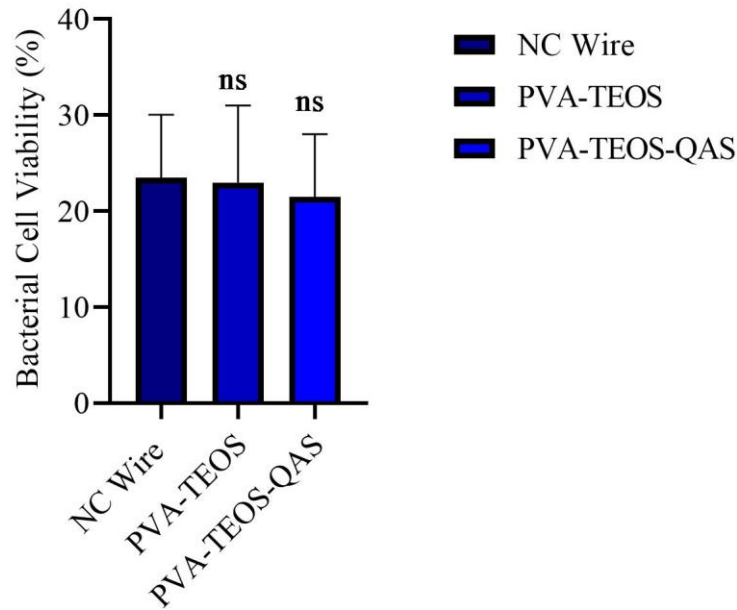


Figure 3. 12: Viability of adhered *S. aureus* cells on K-Wires coated with as determined NC Wire, PVA-TEOS, PVA-TEOS-QAS by Alamar Blue assay. (p value style: GP: 0,1234 (ns), 0,0332(\*), 0,0021(\*\*), 0,0002(\*\*\*), <0,0001(\*\*\*\*))

### 3.2.2 Investigation of *In vitro* Antibiofilm Effect

The capacity of biomaterials to inhibit *S. aureus* biofilm formation was tested using the Resazurin assay for bacterial cell metabolic activity and crystal violet for inhibition of biofilm formation. Crystal violet was chosen due to its ability to bind to negative charges, making it effective against a wide range of bacteria and EPS molecules. Figure 3.13 show that there was no significant difference in reducing biofilm viability between uncoated wires and PVA-TEOS, PVA-TEOS-QAS coated wires.

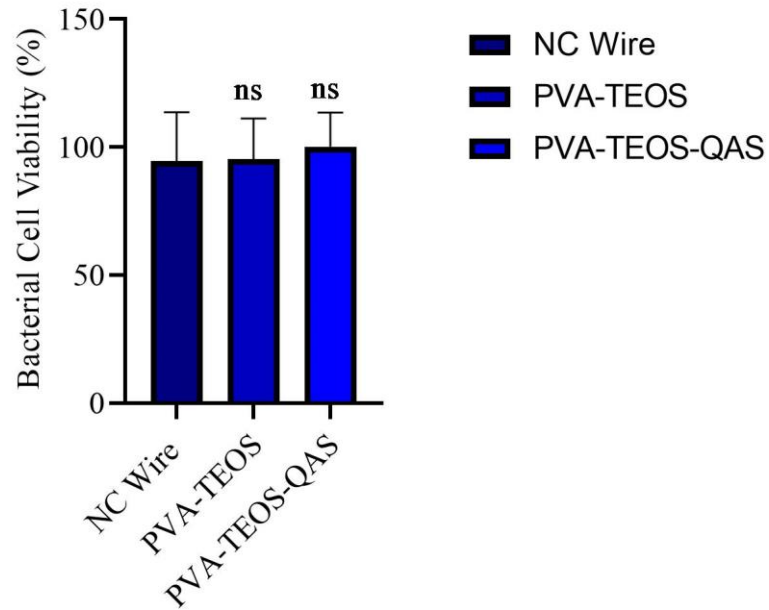


Figure 3. 13: The bacterial cell viability of formed *S. aureus* biofilm on NC Wire, PVA-TEOS, PVA-TEOS-QAS was determined by Alamar blue assay. (p value style: GP: 0,1234 (ns), 0,0332(\*), 0,0021(\*\*), 0,0002(\*\*\*), <0,0001(\*\*\*\*))

Figure 3.14 shows that there was no significant reduction in biofilm biomass between uncoated wires and wires coated with PVA-TEOS or PVA-TEOS-QAS. Therefore, there was no significant effect in inhibiting bacterial biofilm formation for either coating type.

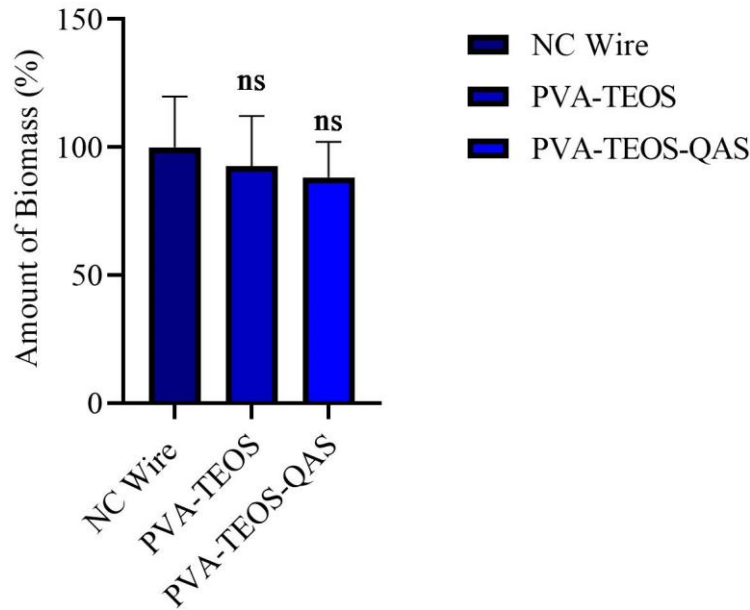


Figure 3. 14: The effect of biomass of *S. aureus* biofilm on NC Wire, PVA-TEOS, PVA-TEOS-QAS was determined with Crystal Violet. (p value style: GP: 0,1234 (ns), 0,0332(\*), 0,0021(\*\*), 0,0002(\*\*\*), <0,0001(\*\*\*\*))

### 3.2.3 *In vitro* Cytocompatibility Results

Cell viability testing was performed according to ISO 10993-5 standards using literature as reference. The cells were incubated until they reached 80% density and extracts were added at 100%, 50%, and 25%. After 24 hours of incubation, the Alamar Blue test was used to analyze cell viability. Statistical analysis was performed using GraphPad Prism 8.4.2. One-way ANOVA was used to determine the P values. The P values were reported as follows: GP: 0.1234 (not significant), 0.0332 (\*), 0.0021 (\*\*), 0.0002 (\*\*\*), and <0.0001 (\*\*\*\*). According to the ISO 10993-5 standard, values below 70% are considered toxic. Figure 3.15 shows that, in three different groups, cell viability does not fall below 70% at different extraction percentages, despite decreases compared to the control in the picture. This indicates that it is not toxic [59].

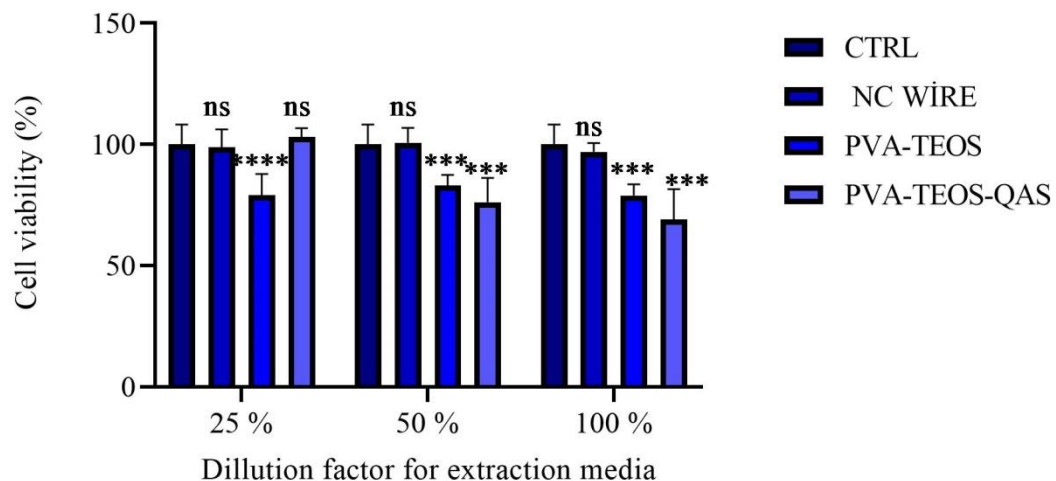


Figure 3. 15: NC Wire, PVA-TEOS, PVA-TEOS-QAS toxicity tests were performed with L929 cell line and cell viability testing was performed with Alamar blue assay. (p value style: GP: 0.1234 (ns), 0.0332(\*), 0.0021(\*\*), 0.0002(\*\*\*), <0.0001(\*\*\*\*))

# Chapter 4

## 4. Conclusion

The sol-gel technique's dip coating method successfully coated the surface of K-Wires. The addition of PVA to the coating matrix enabled a homogeneous and void-free coating. Bactericidal activity against bacteria was achieved using QASs. After coating the K-wires with PVA-TEOS and PVA-TEOS-QAS matrices, which were prepared to provide an antibacterial effect but do not have antibacterial properties by nature, characterization processes were carried out. The study found that the antibacterial coating was effective against *S. aureus* but had no significant impact on biofilm formation. The PVA-TEOS-QAS coating matrix demonstrated a reduction of approximately 55% in bacteria. The material was determined to be non-toxic and compliant with ISO standards, with a viability rate of no less than 70%. The antibacterial coatings produced exhibit short-term bactericidal and bacteriostatic effects. The use of K-Wires in external implants has become a promising approach due to their preference for short-term use. Our future objective is to provide antibacterial and antibiofilm inhibition by prioritising AMP for bacterial species that cause infections associated with K-Wires.

## References

- [1] Tranquillo E, Bollino F. Surface Modifications for Implants Lifetime extension: An Overview of Sol-Gel Coatings. *Coatings* 2020; 10: 589.
- [2] Coatings | Free Full-Text | Surface Modifications for Implants Lifetime extension: An Overview of Sol-Gel Coatings, <https://www.mdpi.com/2079-6412/10/6/589> (accessed 17 January 2024).
- [3] Tiwari SK, Mishra T, Gunjan MK, et al. Development and characterization of sol-gel silica-alumina composite coatings on AISI 316L for implant applications. *Surface and Coatings Technology* 2007; 201: 7582–7588.
- [4] Horkavcová D, Doubet Q, Lecomte-Nana GL, et al. Development of Adhesive, Bioactive and Antibacterial Titania Sol-Gel Coating on Titanium Substrate by Dip-Coating Technique. *Coatings* 2021; 11: 243.
- [5] Combating Implant Infections: Shifting Focus from Bacteria to Host - Amin Yavari - 2020 - Advanced Materials - Wiley Online Library, <https://onlinelibrary.wiley.com/doi/10.1002/adma.202002962> (accessed 17 January 2024).
- [6] Wang R, Shi M, Xu F, et al. Graphdiyne-modified TiO<sub>2</sub> nanofibers with osteoinductive and enhanced photocatalytic antibacterial activities to prevent implant infection. *Nat Commun* 2020; 11: 4465.
- [7] Materials | Free Full-Text | Antibacterial Modification of Kirschner Wires with Polyluteolin toward Methicillin-Resistant Staphylococcus aureus (MRSA), <https://www.mdpi.com/1996-1944/8/8/4876> (accessed 17 January 2024).
- [8] Kim T, See CW, Li X, et al. Orthopedic implants and devices for bone fractures and defects: Past, present and perspective. *Engineered Regeneration* 2020; 1: 6–18.
- [9] Abul A, Karam M, Al-Shammari S, et al. Peri-operative Antibiotic Prophylaxis in K-Wire Fixation: A Systematic Review and Meta-analysis. *JOIO* 2023; 57: 1000–1007.
- [10] Martinez-Perez M, Perez-Jorge C, Lozano D, et al. Evaluation of bacterial adherence of clinical isolates of Staphylococcus sp. using a competitive

model: An in vitro approach to the “race for the surface” theory. *Bone & Joint Research* 2017; 6: 315–322.

- [11] Competitive colonization of prosthetic surfaces by staphylococcus aureus and human cells - Pérez-Tanoira - 2017 - Journal of Biomedical Materials Research Part A - Wiley Online Library, <https://onlinelibrary.wiley.com/doi/10.1002/jbm.a.35863> (accessed 17 January 2024).
- [12] Nanoadhesion of Staphylococcus aureus onto Titanium Implant Surfaces - S. Aguayo, N. Donos, D. Spratt, L. Bozec, 2015, <https://journals.sagepub.com/doi/10.1177/0022034515591485> (accessed 17 January 2024).
- [13] Characterizing the Effect of the Staphylococcus aureus Virulence Factor Regulator, SarA, on Log-Phase mRNA Half-Lives | Journal of Bacteriology, <https://journals.asm.org/doi/10.1128/jb.188.7.2593-2603.2006> (accessed 17 January 2024).
- [14] Oliveira WF, Silva PMS, Silva RCS, et al. Staphylococcus aureus and Staphylococcus epidermidis infections on implants. *Journal of Hospital Infection* 2018; 98: 111–117.
- [15] Bacteria antibiotic resistance: New challenges and opportunities for implant-associated orthopedic infections - Li - 2018 - Journal of Orthopaedic Research - Wiley Online Library, <https://onlinelibrary.wiley.com/doi/10.1002/jor.23656> (accessed 17 January 2024).
- [16] Guo Y, Song G, Sun M, et al. Prevalence and Therapies of Antibiotic-Resistance in Staphylococcus aureus. *Frontiers in Cellular and Infection Microbiology*; 10, <https://www.frontiersin.org/articles/10.3389/fcimb.2020.00107> (2020, accessed 17 January 2024).
- [17] Christaki E, Marcou M, Tofarides A. Antimicrobial Resistance in Bacteria: Mechanisms, Evolution, and Persistence. *J Mol Evol* 2020; 88: 26–40.
- [18] Lei MG, Gupta RK, Lee CY. Proteomics of Staphylococcus aureus biofilm matrix in a rat model of orthopedic implant-associated infection. *PLOS ONE* 2017; 12: e0187981.
- [19] One-year bacterial colonization patterns of Staphylococcus aureus and other bacteria at implants and adjacent teeth - Salvi - 2008 - Clinical Oral Implants Research - Wiley Online Library, <https://onlinelibrary.wiley.com/doi/10.1111/j.1600-0501.2007.01470.x> (accessed 17 January 2024).
- [20] IJMS | Free Full-Text | Colonization and Infection of Indwelling Medical Devices by Staphylococcus aureus with an Emphasis on Orthopedic Implants, <https://www.mdpi.com/1422-0067/23/11/5958> (accessed 17 January 2024).

- [21] Pietrocola G, Campoccia D, Motta C, et al. Colonization and Infection of Indwelling Medical Devices by *Staphylococcus aureus* with an Emphasis on Orthopedic Implants. *International Journal of Molecular Sciences* 2022; 23: 5958.
- [22] Bioengineering | Free Full-Text | Sol-Gel Derived Hydroxyapatite Coatings for Titanium Implants: A Review, <https://www.mdpi.com/2306-5354/7/4/127> (accessed 17 January 2024).
- [23] Ratha I, Datta P, Balla VK, et al. Effect of doping in hydroxyapatite as coating material on biomedical implants by plasma spraying method: A review. *Ceramics International* 2021; 47: 4426–4445.
- [24] Plasma-sprayed CaTiSiO<sub>5</sub> ceramic coating on Ti-6Al-4V with excellent bonding strength, stability and cellular bioactivity | *Journal of The Royal Society Interface*, <https://royalsocietypublishing.org/doi/10.1098/rsif.2008.0274> (accessed 17 January 2024).
- [25] Mechanical, In vitro Antimicrobial, and Biological Properties of Plasma-Sprayed Silver-Doped Hydroxyapatite Coating | *ACS Applied Materials & Interfaces*, <https://pubs.acs.org/doi/10.1021/am201610q> (accessed 17 January 2024).
- [26] Bactericidal activity of biomimetic diamond nanocone surfaces - PubMed, <https://pubmed.ncbi.nlm.nih.gov/26992656/> (accessed 17 January 2024).
- [27] Nanocrystalline hydroxyapatite coatings on titanium: a new fast biomimetic method - ScienceDirect, <https://www.sciencedirect.com/science/article/abs/pii/S0142961204009548?via%3Dihub> (accessed 17 January 2024).
- [28] Bio-surface coated titanium scaffolds with cancellous bone-like biomimetic structure for enhanced bone tissue regeneration - ScienceDirect, <https://www.sciencedirect.com/science/article/abs/pii/S1742706120304104?via%3Dihub> (accessed 17 January 2024).
- [29] Bioinspired and Biomimetic AgNPs/Gentamicin-Embedded Silk Fibroin Coatings for Robust Antibacterial and Osteogenetic Applications | *ACS Applied Materials & Interfaces*, <https://pubs.acs.org/doi/10.1021/acsami.7b06757> (accessed 17 January 2024).
- [30] Osteogenic and antiseptic nanocoating by in situ chitosan regulated electrochemical deposition for promoting osseointegration - ScienceDirect, <https://www.sciencedirect.com/science/article/pii/S0928493118331321?via%3Dihub> (accessed 17 January 2024).
- [31] Electrochemically deposited chitosan/Ag complex coatings on biomedical NiTi alloy for antibacterial application - ScienceDirect, <https://www.sciencedirect.com/science/article/abs/pii/S0257897213004817?via%3Dihub> (accessed 17 January 2024).

- [32] Yahya Rahnamaee S, Bagheri R, Vossoughi M, et al. A new approach for simultaneously improved osseointegration and antibacterial activity by electrochemical deposition of graphene nanolayers over titania nanotubes. *Applied Surface Science* 2022; 580: 152263.
- [33] Coatings | Free Full-Text | Electrochemical Strategies for Titanium Implant Polymeric Coatings: The Why and How, <https://www.mdpi.com/2079-6412/9/4/268> (accessed 17 January 2024).
- [34] Hadzhieva Z, Boccaccini AR. Recent developments in electrophoretic deposition (EPD) of antibacterial coatings for biomedical applications - A review. *Current Opinion in Biomedical Engineering* 2022; 21: 100367.
- [35] Bioactive and antibacterial metal implant composite coating based on Ce-doped nanobioactive glass and chitosan by electrophoretic deposition method | Journal of Materials Research, <https://link.springer.com/article/10.1557/s43578-021-00246-x> (accessed 17 January 2024).
- [36] Hadidi M, Bigham A, Saebnoori E, et al. Electrophoretic-deposited hydroxyapatite-copper nanocomposite as an antibacterial coating for biomedical applications. *Surface and Coatings Technology* 2017; 321: 171–179.
- [37] Bhattacharyya S, Agrawal A, Knabe C, et al. Sol–gel silica controlled release thin films for the inhibition of methicillin-resistant *Staphylococcus aureus*. *Biomaterials* 2014; 35: 509–517.
- [38] A biocompatible sol–gel derived titania coating for medical implants with antibacterial modification by copper integration | *AMB Express* | Full Text, <https://amb-express.springeropen.com/articles/10.1186/s13568-018-0554-y> (accessed 17 January 2024).
- [39] The antimicrobial activity and biocompatibility of a controlled gentamicin-releasing single-layer sol-gel coating on hydroxyapatite-coated titanium | *Bone & Joint*, <https://boneandjoint.org.uk/Article/10.1302/0301-620X.103B3.BJJ-2020-0347.R1> (accessed 17 January 2024).
- [40] A review: Recent advances in sol-gel-derived hydroxyapatite nanocoatings for clinical applications - Choi - 2020 - *Journal of the American Ceramic Society - Wiley Online Library*, <https://ceramics.onlinelibrary.wiley.com/doi/full/10.1111/jace.17118> (accessed 17 January 2024).
- [41] Sol–Gel-Derived Bioactive and Antibacterial Multi-Component Thin Films by the Spin-Coating Technique | *ACS Biomaterials Science & Engineering*, <https://pubs.acs.org/doi/10.1021/acsbomaterials.0c01140> (accessed 17 January 2024).
- [42] Catauro M, Bollino F, Giovanardi R, et al. Modification of Ti6Al4V implant surfaces by biocompatible TiO<sub>2</sub>/PCL hybrid layers prepared via sol-gel dip

coating: Structural characterization, mechanical and corrosion behavior. *Materials Science and Engineering: C* 2017; 74: 501–507.

- [43] Horkavcová D, Novák P, Fialová I, et al. Titania sol-gel coatings containing silver on newly developed TiSi alloys and their antibacterial effect. *Materials Science and Engineering: C* 2017; 76: 25–30.
- [44] Catauro M, Papale F, Bollino F. Characterization and biological properties of TiO<sub>2</sub>/PCL hybrid layers prepared via sol-gel dip coating for surface modification of titanium implants. *Journal of Non-Crystalline Solids* 2015; 415: 9–15.
- [45] SUGUMARAN DrS, Bellan C, Nadimuthu D. Characterization of composite PVA–Al<sub>2</sub>O<sub>3</sub> thin films prepared by dip coating method. *Iranian Polymer Journal*; 24. Epub ahead of print 6 January 2015. DOI: 10.1007/s13726-014-0300-5.
- [46] Muppalaneni S. Polyvinyl Alcohol in Medicine and Pharmacy: A Perspective: *Journal of Developing Drugs*; 02. Epub ahead of print 1 January 2013. DOI: 10.4172/2329-6631.1000112.
- [47] Elena P, Miri K. Formation of contact active antimicrobial surfaces by covalent grafting of quaternary ammonium compounds. *Colloids Surf B Biointerfaces* 2018; 169: 195–205.
- [48] Poverenov E, Shemesh M, Gulino A, et al. Durable contact active antimicrobial materials formed by a one-step covalent modification of polyvinyl alcohol, cellulose and glass surfaces. *Colloids and Surfaces B: Biointerfaces* 2013; 112: 356–361.
- [49] Daood U, Burrow MF, Yiu CKY. Effect of a novel quaternary ammonium silane cavity disinfectant on cariogenic biofilm formation. *Clin Oral Investig* 2020; 24: 649–661.
- [50] Gong S, Niu L-N, Kemp LK, et al. Quaternary ammonium silane-functionalized, methacrylate resin composition with antimicrobial activities and self-repair potential. *Acta Biomater* 2012; 8: 3270–3282.
- [51] Bryaskova R, Pencheva D, Kale GM, et al. Synthesis, characterisation and antibacterial activity of PVA/TEOS/Ag-Np hybrid thin films. *Journal of Colloid and Interface Science* 2010; 349: 77–85.
- [52] Daood U, Parolia A, Elkezza A, et al. An in vitro study of a novel quaternary ammonium silane endodontic irrigant. *Dental Materials* 2019; 35: 1264–1278.
- [53] Tranquillo E, Bollino F. Surface Modifications for Implants Lifetime extension: An Overview of Sol-Gel Coatings. *Coatings* 2020; 10: 589.
- [54] Bouloussa H, Saleh-Mghir A, Valotteau C, et al. A Graftable Quaternary Ammonium Biocidal Polymer Reduces Biofilm Formation and Ensures Biocompatibility of Medical Devices. *Advanced Materials Interfaces* 2021; 8: 2001516.

- [55] van de Lagemaat M, Grotenhuis A, van de Belt-Gritter B, et al. Comparison of methods to evaluate bacterial contact-killing materials. *Acta Biomaterialia* 2017; 59: 139–147.
- [56] Peralta JM, Meza BE, Zorrilla SE. Mathematical Modeling of a Dip-Coating Process Using a Generalized Newtonian Fluid. 1. Model Development. *Ind Eng Chem Res* 2014; 53: 6521–6532.
- [57] KALAMPOUNIAS AG. IR and Raman spectroscopic studies of sol–gel derived alkaline-earth silicate glasses. *Bull Mater Sci* 2011; 34: 299–303.
- [58] Sandberg M, Määttänen A, Peltonen J, et al. Automating a 96-well microtitre plate model for *Staphylococcus aureus* biofilms: an approach to screening of natural antimicrobial compounds. *Int J Antimicrob Agents* 2008; 32: 233–240.
- [59] Jablonská E, Kubásek J, Vojtěch D, et al. Test conditions can significantly affect the results of in vitro cytotoxicity testing of degradable metallic biomaterials. *Sci Rep* 2021; 11: 6628.
- [60] Zhang S, Liang X, Gadd GM, et al. A sol–gel based silver nanoparticle/polytetrafluorethylene (AgNP/PTFE) coating with enhanced antibacterial and anti-corrosive properties. *Applied Surface Science* 2021; 535: 147675.
- [61] Kügler R, Bouloussa O, Rondelez F. Evidence of a charge-density threshold for optimum efficiency of biocidal cationic surfaces. *Microbiology (Reading)* 2005; 151: 1341–1348.
- [62] Permanent, non-leaching antibacterial surfaces—2: How high density cationic surfaces kill bacterial cells - ScienceDirect, <https://www.sciencedirect.com/science/article/pii/S0142961207004681> (accessed 17 January 2024).
- [63] Eliaz N, Shmueli S, Shur I, et al. The effect of surface treatment on the surface texture and contact angle of electrochemically deposited hydroxyapatite coating and on its interaction with bone-forming cells. *Acta Biomaterialia* 2009; 5: 3178–3191.
- [64] Xu X, Wang H, Zhang S, et al. ECM-inspired 3D printed polyetherimide scaffold with Arg-Gly-Asp peptides for the improvement of bioactivity and osteogenic differentiation of osteoblasts. *Materials Today Communications* 2022; 30: 103166.
- [65] Javadi A, Solouk A, Haghbin Nazarpak M, et al. Surface engineering of titanium-based implants using electrospraying and dip coating methods. *Materials Science and Engineering: C* 2019; 99: 620–630.
- [66] Maikranz E, Spengler C, Thewes N, et al. Different binding mechanisms of *Staphylococcus aureus* to hydrophobic and hydrophilic surfaces. *Nanoscale* 2020; 12: 19267–19275.

- [67] Daood U, Burrow MF, Yiu CKY. Effect of a novel quaternary ammonium silane cavity disinfectant on cariogenic biofilm formation. *Clin Oral Invest* 2020; 24: 649–661.
- [68] Şen Karaman D, Karakaplan MB, Erdoğan N. Bacteriostatic Polylactic Acid Coatings Enriched with Zinc Oxide and Silica Nanoparticles for Titanium Pedicle Screws. *JOM* 2021; 73: 4410–4418.





# Appendices

# Appendix B

## Publications from the Thesis

### Conference Papers

1. BAKTERİYEL HÜCRE KÜLTÜRÜ ORTAMINDA FİZİKOKİMYASAL KARAKTERİSTİK ANALİZİ İLE SERYUM OKSİT NANOPARTİKÜLLERİNİN ANTİBAKTERİYEL MEKANİZMASININ AYDINLATILMASI: 2. INTERNATIONAL ULUDAĞ SCIENTIFIC RESEARCHES CONGRESS (04-05 NOVEMBER 2023 BURSA/TÜRKİYE)

# Curriculum Vitae

Name Surname : Emine Hilal Altıntop

## Education:

2012–2017 Karabük University, Dept. of Biomedical Eng.

2021–2024 İzmir Kâtip Çelebi University, Dept. of Biomedical Eng.

.